



TALLINN UNIVERSITY OF TECHNOLOGY

SCHOOL OF ENGINEERING

Department of Electrical Power Engineering and Mechatronics

# **DESIGN OPTIMIZATION OF SOLAR-POWERED THERMOELECTRIC GENERATOR THERMAL COLLECTOR**

## **PÄIKESEENERGIA TOITEL TERMOELEKTRIGENAATORI SOOJUSKOLLEKTORI KONSTRUKTSIOONI OPTIMEERIMINE**

MASTER THESIS

Student: Ubaid Fayaz

Student code: 195426MAHM

Supervisor: Professor Lauri Kütt

Tallinn 2021

(On the reverse side of title page)

## **AUTHOR'S DECLARATION**

Hereby I declare, that I have written this thesis independently.  
No academic degree has been applied for based on this material. All works, major viewpoints and data of the other authors used in this thesis have been referenced.

"10" June 2021

Author: .....  
*/signature /*

Thesis is in accordance with terms and requirements

"....." ..... 20....

Supervisor: .....  
*/signature/*

Accepted for defence

"....." .....20... .

Chairman of theses defence commission: .....  
*/name and signature/*

## **Non-exclusive Licence for Publication and Reproduction of Graduation Thesis<sup>1</sup>**

I, Ubaid Fayaz (date of birth: 20/12/1993) hereby

1. grant Tallinn University of Technology (TalTech) a non-exclusive license for my thesis DESIGN OPTIMIZATION OF SOLAR-POWERED THERMOELECTRIC GENERATOR THERMAL COLLECTOR,

supervised by

Professor Lauri Kütt,

1.1 reproduced for the purposes of preservation and electronic publication, incl. to be entered in the digital collection of TalTech library until expiry of the term of copyright;

1.2 published via the web of TalTech, incl. to be entered in the digital collection of TalTech library until expiry of the term of copyright.

1.3 I am aware that the author also retains the rights specified in clause 1 of this license.

2. I confirm that granting the non-exclusive license does not infringe third persons' intellectual property rights, the rights arising from the Personal Data Protection Act or rights arising from other legislation.

---

<sup>1</sup> *Non-exclusive Licence for Publication and Reproduction of Graduation Thesis is not valid during the validity period of restriction on access, except the university's right to reproduce the thesis only for preservation purposes.*

\_\_\_\_\_ (signature)

10/06/2021

Department of Electrical Power Engineering and Mechatronics

**THESIS TASK**

**Student:** Ubaid Fayaz, 195426MAHM

Study programme, MAHM02/18 - Mechatronics

main speciality: Mechatronics

Supervisor(s): Professor Lauri Kütt, 6203806

Consultants: .....(name, position)

..... (company, phone, e-mail)

**Thesis topic:**

(in English) DESIGN OPTIMIZATION OF SOLAR-POWERED THERMOELECTRIC GENERATOR THERMAL COLLECTOR

(in Estonian) PÄIKESEENERGIA TOITEL TERMOELEKTRIGENAATORI SOOJUSKOLLEKTORI KONSTRUKTSIOONI OPTIMEERIMINE

**Thesis main objectives:**

1. Design optimization of a solar thermoelectric generator assembly
2. Minimizing the heat leakage
3. Selection of the insulation material

**Thesis tasks and time schedule:**

No	Task description	Deadline
1.	Information search and review of previous work	19.01.2021
2.	Developing designs and simulation on ANSYS	March 2021
3.	Fabrication and test the optimized model	April 2021
4.	Thesis defence	June 2021

**Language:** English

**Deadline for submission of thesis:** 10/06/2021

**Student:** Ubaid Fayaz .....  
/signature/

**Supervisor:** Lauri Kütt .....  
/signature/

**Head of study programme:** ..... "....." .....2021

*Terms of thesis closed defence and/or restricted access conditions to be formulated on the reverse side.*

## **Table of content**

Table of figures .....	7
Table of tables.....	8
PREFACE .....	9
ABSTRACT.....	10
List of abbreviations and symbols.....	12
1 INTRODUCTION .....	13
2 LITERATURE REVIEW AND BACKGROUND.....	16
2.1 Existing Methods .....	16
2.2 Conclusion.....	23
2.3 Objective of the Thesis .....	24
3 CONCEPTS OF HEAT TRANSFER.....	26
3.1 Conduction.....	26
3.2 Convection .....	27
3.3 Radiation .....	28
3.4 Validation with the empirical solution.....	28
3.5 Methodology.....	30
4 ABSORBER'S INSULATION DESIGN.....	33
4.1 Meshing.....	35
4.2 Different boundary conditions and enclosure .....	36
4.3 Simulation results .....	36
4.4 Base for optimization.....	38
5 FABRICATION AND TESTING.....	40
5.1 Previous and currently used and tested insulating material.....	40
5.1.1 Fire-resistant foam .....	40
5.1.2 Stone wool.....	41
5.1.3 Ceramic fibre wool.....	41
5.1.4 Currently used calcium silicate material.....	41
5.2 Heat source part.....	42
5.3 Temperature sensors.....	43

5.4 Fabrication of a robust assembly.....	44
5.4.1 More robust and adjustable alterations .....	45
5.5 Power supply.....	46
5.6 Data acquisition software and device .....	47
6 TESTING .....	49
6.1 Comparison base for testing.....	49
6.1 Thermal leakage and build quality .....	50
6.2 Testing of fully covered assembly .....	50
6.3 Testing completely open gap at the bottom (adding emission).....	52
6.5 Partially open gap testing (emission evaluation).....	56
7 RESULTS ANALYSIS .....	57
7.1 Iterations to match Ansys simulations for thermal conductivity ...	57
7.2 Iterations in Ansys simulations for emissivity .....	58
8 TEG ADAPTER PROPOSAL.....	62
8.1 Previously used adapter .....	62
8.2 Adapter redesigned .....	62
8.3 Adapter simulation .....	63
9 CONCLUSION.....	65
10 JÄRELDUSED .....	66
LIST OF REFERENCES .....	67

## Table of figures

Figure 1.1 Parabolic Dish .....	13
Figure 2.1 Schematic of the STEG prototype of Olsen et al. Research .....	20
Figure 2.2 Different orientation of solar cavity [19] .....	23
Figure 3.1 Conduction, convection and radiation illustration .....	26
Figure 3.2 The temperature gradient across the plate .....	30
Figure 3.3 Ansys workbench modules .....	32
Figure 4.1 Description of absorber's insulation .....	33
Figure 4.2 Absorber's meshing .....	35
Figure 4.3 Mesh size examples .....	36
Figure 4.4 Different boundary conditions .....	37
Figure 4.5 Results of thermal losses in different simulated models .....	38
Figure 4.6 Most optimum dimensions .....	39
Figure 5.1 Heated plate .....	42
Figure 5.2 Heated plate circuit .....	43
Figure 5.3 Temperature sensors .....	44
Figure 5.4 fabricated assembly .....	45
Figure 5.5 More adjustable outer frame .....	46
Figure 5.6 Power supply .....	46
Figure 5.7 Power supply user interface .....	47
Figure 5.8 Keysight data acquisition device .....	48
Figure 5.9 BenchLink data logger .....	48
Figure 6.1 Thermal camera contours .....	50
Figure 6.2 Power vs temperature graph .....	52
Figure 6.3 Illustration of the open gap at the bottom .....	53
Figure 6.4 Support at different angles .....	55
Figure 7.1 Thermal conductivity specification flow chart .....	57
Figure 7.2 Emissivity flow chart .....	59
Figure 7.3 Input power vs temperature .....	60
Figure 8.1 Absorber .....	63
Figure 8.2 Rectangular plates .....	64
Figure 8.3 Cone shaped plates .....	64

## Table of tables

Table 3.1 Mechanical properties of the Skamotec material .....	29
Table 3.2 Chemical composition of Skamotec insulating material. ....	29
Table 4.1 Following models are the sequence of the absorber’s geometry which is being modified: .....	34
Table 4.2 Ansys simulations for design optimization .....	39
Table 5.1 Properties of previously used insulating materials .....	40
Table 6.1 Different boundary conditions on different enclosures: .....	49
Table 6.2 Power against temperature .....	51
Table 6.3 Second and third assembly, power against temperature .....	51
Table 6.4 Fully open gap at the bottom .....	54
Table 6.5 Fully open gap at different angles .....	55
Table 6.6 Partially filled gap .....	56
Table 7.1 Prototype power vs Ansys power for thermal conductivity .....	58
Table 7.2 Prototype power vs Ansys power for emissivity .....	59
Table 7.3 Trend x and trend constant of heat transfer at angles .....	60



## **PREFACE**

First of all, I would like to express my deepest gratitude to God for making all this possible, and also gave me the privilege of completing this thesis.

From the core of my heart, I would like to thanks to my supervisor, Lauri Kütt, Professor at Tallinn University of Technology for giving me the support and opportunity to do my research work, I say thank you.

My utmost gratitude goes to my loving parents Mr. and Mrs. Fayaz Iqbal, for trusting and permitting me to do my master's program in Estonia and to both of my siblings Junaid Fayaz, and Anam Fayaz for being my support. I would also acknowledge and say thank you to the better half of my life, Hamna Nadeem, for giving me moral support and time to work on my thesis.

Finally, Obaid Anwar, Hafiz ul Islam, Farhad, Kakajan, Wali Khan, Kaleem Ullah, and Waqas Rashid, to all my pals. Thank you for all of your profound help, contributions, and encouragement throughout this thesis's development. Thank you very much.

The goal of this research is to improve the design of a solar-powered thermoelectric generator thermal collector. Its goal is to use simulations, fabrication, and testing to investigate the design optimization of a thermoelectric generator assembly.

## **ABSTRACT**

The engineering problem in establishing thermoelectric generator (TEG) high and cold temperature sites is that the energy in the high temperature side sinks towards the cold temperature side, driving the whole system to the equilibrium. This sink of the energy to the cold temperature side through TEG systems thermal system parts to the ambience of the hot side components results in the plummet of the overall efficiency. One of the solutions to improve the thermal system efficiency is to use a thermal cavity type design.

In this research study, TEG system hot side components were investigated. Several simulations were performed to establish the optimum design parameters of the assembly. ANSYS simulation environment is used to apply the finite element method. With the help of simulations results, conduction, convection and radiation are the three types of heat transfer that were calculated in the simulations. Further simulations were performed for the calculation of the different configurations of the whole assembly. The whole assembly is simulated for the fully covered, partially covered, and fully open gap of the thermal cavity type enclosure.

To verify the results, the most optimum designated proposal through the simulations was fabricated in the workshop. The insulating material used in the simulations built with main objective in fabrication to provide such an intact assembly that the heat leakage is minimum.

Testing strategy to verify the simulation and analysis results was by use of electric heating to stimulate solar power input to potential TEG system. Heated part with target function of solar absorber was fitted into isolation parts. To evaluate the insulation performance the heated part testing was performed for several input powers. The testing was done on all the three configurations, fully and partially open gap and fully closed gap to measure the temperature of the heated plates. In real usage of the assembly, it will be positioned at different angles so that is why the prototype is also tested for different angles as well.

The result of this thesis shows that still further studies would be needed for improving the results.

**Keywords:** Thermoelectric generator, Ansys, thermal insulation, temperature measurement, conduction, convection, radiation, heat transfer

## Resümee

Termoelektrilise elemendiga seotud kõrge ja madala temperatuuri alade kujundamise inseneriülesanne arvestada paratamatu soojuslekkega kuumalt poolelt külmale, ühtlustades süsteemi temperatuuri. Kuumal poolel oleva energia otseliikumisel külmale poolele ja ümbritsevasse keskkonda langeb üldist kasutegurit. Üks lahendus soojussüsteemi kasuteguri tõstmiseks on kasutada soojuskambri tüüpi kujundust.

Käesolevas uurimistöös vaadeldi termoelektrilise süsteemi kuuma poole komponente. Optimaalsete kujundusparameetrite leidmiseks viidi läbi arvukalt koostu simulatsioone. Lõplike elementide meetodi rakendamiseks kasutati Ansys keskkonda. Simulatsioonile tuginevalt arvutati kolme soojusülekandeviisi, juhtivusliku soojusülekande, soojuskiirguse ja konvektiivse ülekande suurused. Täiendavalt vaadeldi simulatsioonil kogu koostu erinevaid konfiguratsioone. Koostu on uuritud lähtudes soojuskambri oleva ava puudumisel, täielikult kaetud, osaliselt kaetud ja täielikult avatud vahega.

Tulemuste kinnitamiseks ehitati Tehnikaülikooli töökodades valmis koostu kujundus, milline oli simulatsioonidel kinnitatud kui kõige optimaalsem. Kasutati sama isolatsioonimaterjali kui simulatsioonidel ja koostu ehitamisel seati sihiks erinevate soojuslekete minimeerimine.

Katsetamise põhimõtteks oli simulatsiooni- ja analüüsitulemuste kinnitamine läbi elektrilise kuumutamise, mis simuleeriks päikeseenergia neeldumist termoelektrilise süsteemi kuumal poolel. Päikeseneeldurit esindav kuumutatud alamosa paigutati soojusisolatsiooniosade vahele. Soojusisolatsiooni tõhususe hindamiseks katsetati kuumutatud alamosa erinevatel kuumutusvõimsuste tasemetel. Katsed viidi läbi kõigis kolmes seadistuses, soojuskambri ava täielikult ja osaliselt avatuna ja täielikult suletuna, mõõtes kuumutatud osa lõpptemperatuuri. Koostu potentsiaalses lõppkasutuses on ette näha erineva nurga all paiknemist, seetõttu ka prototüüpi katsetatakse erinevates asendites erinevate paigutusnurkade korral.

Lõputöös esitletud tulemused osutavad, et on vaja täiendavat uurimistööd tulemuste parendamiseks.

**Võtmesõnad:** Termoelektriline generaator, Ansys, soojusisolatsioon, temperatuurimõõtmised, soojusjuhtivus, soojuskiirgus, konvektsioon, soojusülekanne

## **List of abbreviations and symbols**

TEG – Thermoelectric Generator

FEM – Finite Element Method

FEA – Finite Element Analysis

AOA – Angle of Attack

Re – Reynolds number

CPM - Critical Path Method

ZT – Figure of Merit

NREL – National Renewable Energy Laboratory

HFSF – High Flux Solar Furnace

CTG – Concentration solar thermoelectric generator

CFD – Computational fluid dynamics

TEC-TEG – Thermoelectric cooler-thermoelectric generator

# 1 INTRODUCTION

The thermoelectric generator (TEG) is a device that consists of semiconductors and metal conductors. The semiconductor in the TEG is sandwiched between two heat conductive plates. The working phenomenon of the thermoelectric generator is based on the temperature gradient on both sides of the TEG. One of the plates is attached to the high temperature and the other is attached to the low temperature site. Due to this temperature gradient, electrons and holes are produced in the semiconductor which in turn causes the voltage and electric current. High temperature can be provided to the TEG by different heat sources and on the other hand, a low-temperature side can be achieved by attaching the TEG with the water-cooled heat exchanger.

In this research scope, a concentrated solar is considered heat energy as an input energy source. This solar heat energy can be extracted with the parabolic solar dish concentrator. With the help of a parabolic dish, the radiation from the sun is concentrated to one point above the dish and the heat is provided to the TEG on one side. The target temperature on the high-temperature side is 300 °C. The other side of the TEG is attached to the water- and air-cooled heat exchanger which is 20 °C to 40 °C.

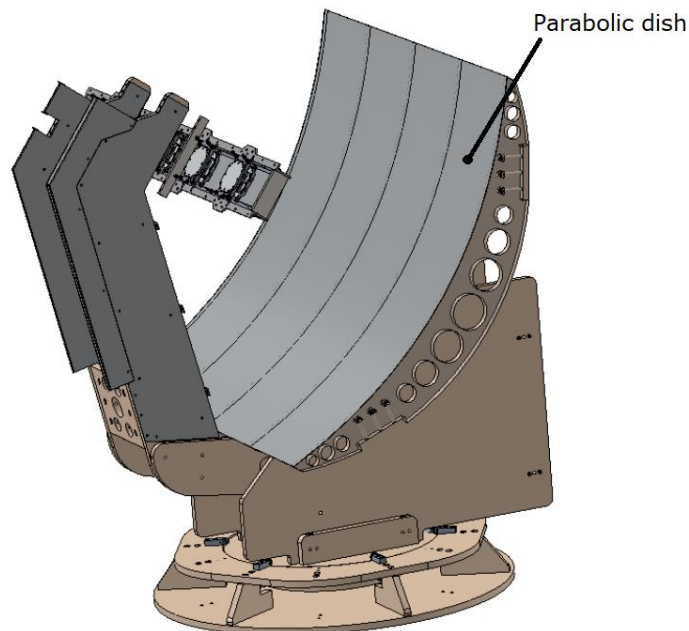


Figure 1.1 Parabolic dish TEG system proposal

The engineering problem in this kind of assemblies are that heat energy for the higher temperature side is leaked to the lower temperature side only because of the thickness of the TEG. The thickness of TEG is so small that heat transfer from a higher temperature

side to the lower temperature side is too difficult to fully eliminate. Looking at this constraint, it can be optimized by redesigning the model and choosing the optimum insulating material. To summarize the whole solution idea, by optimizing the design, it is possible to minimize the heat leakage which will, in turn, increase efficiency. The optimum design has a huge and varying significance in the world of engineering. The design can not only be used with a solar dish concentrator but can also be used wherever TEG is being used.

According to the current situation on the topic, there isn't much material on the design optimization of TEG setup assembly. It has been observed that most of the research is being done on the thermoelectric materials to produce the maximum output and an increased life span of the material. In most of the research work on TEG, only a temperature gradient is provided to the TEG without any design optimization of the assembly that holds it.

This master's thesis research revolves around the concept to redesign the TEG's assembly so that there are minimum heat leakages. To pursue the research, practical and theoretical approaches are being followed. Practically, this research will produce results by working on a prototype, and theoretically, simulations of thermal analysis will be performed using ANSYS. Previously, prototypes have already been built in the laboratory but the insulating material which was being used was not the optimum material. In the design and research area, choosing optimum insulating material is also a part. For the best design and insulating material selection, the literature review is one of the key features in this research.

In this master's thesis research, focus is on the finite element method for the optimized design of TEG assembly and by using manufacturing processes, prototype will be fabricated of a proposed design. After manufacturing the prototype, physical tests will be performed on that assembly by applying heat and measuring the temperature on different surfaces of the prototype. With the help of the finite element method, the selection of the best insulating material will also be simulated and applied to the manufactured and finalized design of the TEG assembly. Initially, the proposed design will be visualized to a 3D model using Solidworks and alterations will also be made in the same 3D model to optimize the whole design. The model will also be made in consideration of available additive manufacturing technologies in our university. For thermal analysis of the design, ANSYS is one of the most used tools among researchers and scientists. ANSYS is well-known due to its up-to-date versions and a wide range of

modules, for instance, static structural to explicit dynamics and computational fluid dynamic CFX to thermal analysis.

As far as measuring the success of the research is concerned, the minimum heat leakage and greater temperature gradient are the scales for the successful research. The goal is to achieve a design that can offer minimum leakage of heat from the high-temperature side to the low-temperature side. Another study is about the selection of the insulating material which will be used in an efficient way to make the whole TEG assembly work better. The results from FEM cannot be perfect the same as the results or numbers from physically testing the prototype because of the tolerances and computational ideal construction.

## **2 LITERATURE REVIEW AND BACKGROUND**

### **2.1 Existing Methods**

In recent years, the use of alternative energy methods has increased due to the environmental impact produced, mostly, by fossil fuel. The use of solar energy has been prominent in this scenario, thus, scholars around the world have devoted a great effort to the invention of new technologies for use of solar energy. The main purpose of finding new methods is to reduce the carbon footprint and to meet the increasing energy demands. These new methods which are ingeniously combined such as TEG combined with the parabolic dish need optimization in their design to enhance their performance. The method of optimization of any design in this era is based on using experimental data collection or using the simulation techniques by using software packages.

In 1888, Weston [1], took help from a black surface painted for the absorption of the solar radiation onto a thermoelectric module to patent a device. Severy [2-3] presented a STEG that had a pump for supplying the cold water to the cold side of the module, a tracking device, and a battery. Coblenz [4], patented the STEG with a hot side temperature of 100 °C with his first experimental results, but the experimental efficiency was not recorded.

In the journal article of Dongxu Ji [5], the design focuses on heat waste recovery from automotive and marine engines. The research implements a framework for the design of thermoelectric generators around the exhaust of the automotive and marine engines to convert waste heat energy to electrical energy. In his article, one of the robust designs has been proposed by Genichi Taguchi. Taguchi method has been used to improve the quality of mechanical manufacturing goods. The following five design parameters have been considered for the analysis of waste heat recovery from marine and automotive engines, (i) the fill ratio, (ii) ratio of the cross-sectional area of n-type material over p-type material of the thermoelectric module, (iii) height, (iv) length, (v) the material of the heat exchanger. The contribution of these design parameters is 69,9% and 30,25% in automotive and marine applications, respectively.

One of the bio-inspired designs in order to find optimum values of design parameters of a heat sink having hexagonal cells were exactly like the honeycomb cells. The article [6] discusses the failure of electronic devices that depend mostly on the temperature, this is the reason the researcher worked on the heat sink of electronic devices. The main



design idea is inspired by the structure of the honeycomb which is not only durable but also well ventilated. In this research work, several parameters have been used such as Angle of attack (AOA), fin thickness, fin height, Reynolds number (Re), and longitudinal pitch are chosen as design variables while the factor of friction and Nusselt number is chosen as the objective function. In this thesis research work, this heat sink design could be used in order to keep the low-temperature side of the TEG at low temperatures.

In 2011 the results of Telkes were tested by Kraemer [7] who experimentally demonstrated 4,6% efficiency in a Bi<sub>2</sub>Te<sub>3</sub> nanostructured STEG. To minimize conductive and convective losses, a vacuum enclosure was used, and selective absorbers were used as a thermal concentrator in the design. In 2011, a paper by Chen [8] used a constant property model (CPM) approach to indicate the important variables in the design. In this study, the author emphasized increasing the efficiency of the STEG by using a selective absorber to get the most out of the net flux into the thermal concentrator. He also focuses on the applications of an evacuated tube used by the solar-thermal steam plant and solar hot-water systems and said that these systems are realistic and economically feasible.

A paper by McEnaney [9], states that finite element modelling (FEM) was used for the determination of the predicted device performance for a thermoelectric material and specified generator design. As photovoltaic systems and concentrating solar dishes and troughs, solar thermoelectric generators (STEG's) also generate electricity by sunlight. STEGs work by absorbing solar energy, which generates a temperature difference, that helps to generate electricity through the Seebeck effect in the thermoelectric device. The efficiency of a STEG thus depends on both the efficiency of the solar device with which sunlight is converted to heat and on the thermoelectric efficiency. The thermoelectric efficiency of thermoelectric material is expressed by the dimensionless thermoelectric figure of merit (ZT), which is dependent on the transport properties of the material as shown in the following equation.

$$ZT = \frac{S^2 \sigma T}{K} \quad (2.1)$$

where  $S$  - Seebeck coefficient,  $\mu\text{V}/\text{K}$ ,

$\sigma$  - electrical conductivity,  $1/\Omega \text{ m}$ ,

$K$  - thermal conductivity,  $\text{W}/\text{m K}$ .

The postulates below should be met in order to maximize the ZT of a material:

- To maintain low thermal conductivity and a considerable temperature difference between both sides of the material
- To keep high electrical conductivity in order to diminish the internal resistance of the material and the Joule effect.
- High Seebeck coefficient, compulsory to obtain a high voltage.

The graph of the figure of the merit  $ZT$  shows that, unfortunately, the parameters are much associated with each other and it not a piece of cake to optimize them independently, mostly in the case of conventional metals.

The maximum efficiency [10] of a TEG is given by.

$$\eta_{TE} = \left(1 - \frac{T_c}{T_h}\right) \frac{\sqrt{1+Z\bar{T}}-1}{\sqrt{1+Z\bar{T}+\frac{T_c}{T_h}}} \quad (2.2)$$

where  $\eta_{TE}$  – efficiency of a TEG, %,

$T_c$  – cold side temperature, K,

$T_h$  – hot side temperature, K.

The first term of the equation described above is the Carnot efficiency. For the efficiency of a thermoelectric generator (TEG), the ratio between the electrical power produced and the heat flow through the module must be calculated. These standard equations rely on four conditions known as (i) the electrical and thermal contact resistances are insignificant, (ii) the Thomson effect has almost no effect on efficiency, (iii) losses due to convection and radiation are negligible, and (iv) the dependence on the thermoelectric transport properties of the TEG module with temperature, which changes the performance of TEGs with respect to the change in temperature.

And the [11] overall efficiency of a combined system is calculated by.

$$\eta = \frac{\text{Electrical energy produced by STEG}}{\text{Solar energy incident on the concentrator}} \quad (2.3)$$

where  $\eta$  – efficiency, %.

$$\eta = \eta_{opt} \times \eta_{therm} \times \eta_{TE} \quad (2.4)$$

where  $\eta_{opt}$  – optical efficiency, %,  
 $\eta_{therm}$  – thermal efficiency, %,  
 $\eta_{TE}$  – thermoelectric efficiency, %.

The absorber surface is not a perfect black body, therefore only a fraction of the incident energy is absorbed ( $q''_{abs}$ ) and the rest is reflected into the atmosphere ( $q''_{inc}$ ). The surface which absorbed energy has a possibility to relate with the total incident energy as following:

$$q_{abs} = A_{abs} \int_0^{\infty} \alpha_s(E) q''_{inc}(E) dE \quad (2.5)$$

where  $\alpha_s$  – spectral absorptivity, W/m<sup>2</sup>,  
 $A_{abs}$  – area of the absorber surface, m<sup>2</sup>.

The optical efficiency depends upon the type of reflector being used, the flux density over the focal area, and the amount of falling radiation is being absorbed. The thermal efficiency of the system, if only the radiation and convection are the main cause of heat loss, is given by.

$$\eta_{therm} = 1 - \frac{\delta(T_h - T_{amb}) + \varepsilon\theta(T_h^4 - T_{amb}^4)}{W_i RC\psi\alpha} \quad (2.6)$$

where  $\eta_{therm}$  – thermal efficiency, %,  
 $\delta$  – convection coefficient of heat transfer, W/(m<sup>2</sup>·K),  
 $\varepsilon$  – emissivity,  
 $\theta$  – Stefan's constant, W/ (m<sup>2</sup>·K<sup>4</sup>),  
 $T_{amb}$  – ambient temperature, K,  
 $W_i$  – solar radiation, Bq,  
 $R$  – reflectivity,  
 $C$  – solar concentration factor,  
 $\alpha$  – wavelength, m.

The energy density flux (W) which is on the hot side of the TEG is.

$$W = W_i RC\psi \quad (2.7)$$

By analysing these equations, it implies that both  $\eta_{opt}$ ,  $\eta_{therm}$  decrease with the increase in operating temperatures, and the  $\eta_{therm}$  increases with the solar concentration factor (C).

Olsen et al. [12], in their research, designed a prototype including a radiation barrier from a jump and redirected it to the lower point. The working principle of the hole is that the sun is fixed centred at the waist and enters through a small hole at the top of the hole. The light varies inside the hole so that to completely illuminate the area of diminution. Any sunlight reflected by the absorber or rays of black light i.e., the above discharge is then (i) shown in the hole, (ii) absorbed and fired by the abscess, or (iii) lost through a hole. Proper selection of hole geometry can increase the chances of exposure and the light will be directed towards the dimming area. Many layers of hole foil are used to improve their performance to protect the practice, increasing the chances of radiation being returned to the pit and deposited with the device rather than the loss of the walls. A hole can be designed so that the opening space is smaller than the melting point of a solid at an angle at which radiation can emit.

Olsen's et al. research concludes that earlier exhibits of the STEG innovation achieved limited efficiencies ( $\sim 5\%$ ) due to the low Carnot effectiveness due to a small temperature drop and the limitations of the ZT for the materials used. To achieve the focused competency, a high ZT thermoelectric device with increased optical fixation and productive solar-powered energy must be built in order to change the heat and create a huge temperature drop across the device. The model plan contains improved solar-selective protective materials and a heat protection hole to ensure a high absorption capacity for sun-driven radiation and at the same time limit the calamity of heat. The test of coupling the required sun-driven fixation to the STEG is met by adjusting the yield of National Renewable Energy Laboratory NREL's High Flux Solar Furnace HFSF.

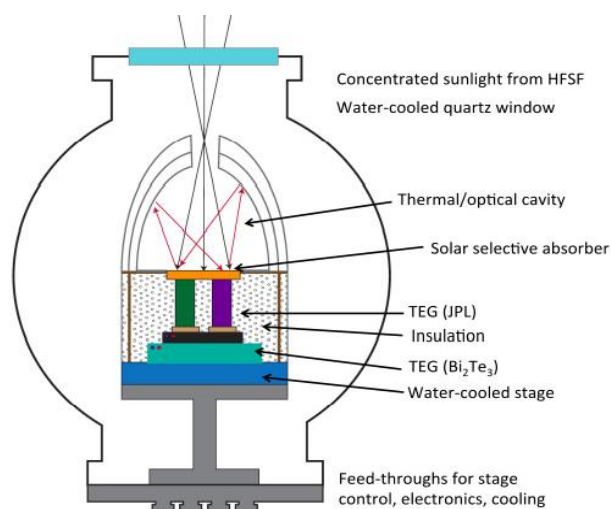


Figure 2.1 Schematic of the STEG prototype of Olsen et al. Research

G. Muthu [13] used experimental data of a prototype, concentrated thermoelectric generator using a parabolic dish and showed the increased performance of TEG by making the heat sink insulated and the receiver plate enclosed in an acrylic cover. In his model, the reflector was made by using triangular pieces of aluminium with a total surface area of 10,53m<sup>2</sup>. The receiver unit which faces the concentrator is coated with black paint to increase absorption and has an area of 0,1m<sup>2</sup>. The heat sink is water-cooled and keeps the temperature as low as possible on the cool side of TEG. He also stated that the optical efficiency of the collector depends on the reflectivity of the concentrator surface and the absorptivity of the receiving surface. The average absorptivity value stated in his research is 0,96 and the reflectance value of aluminium surface is 0,68. The experimental data discussed in his paper states that the maximum temp recorded was 383 K with 1050 W/m<sup>2</sup> of solar radiation and the minimum was 326 K with 600 W/m<sup>2</sup> of radiation. The findings of the research are that a 1,56% higher temperature is obtained by covering the system with respect to a TEG system without cover and a 2,11% improvement in the overall system.

Peng Li's [14] model takes into consideration the temperature dependence of the thermoelectrical material properties by dividing the thermoelectrical leg into finite elements and is tested to be a lot correct for calculation of the conversion efficiency of the thermoelectrical modules once giant temperature gradients occur within the system. The article concludes that an experimental model of a concentrated solar thermoelectric generator is proposed. Compared with usual CTG systems, the design has improved system integrity and reduced system energy losses, which results in increased total conversion potency.

An improved theoretical model of the CTG system is developed to predict system performance based on the simplest offered properties of various bulk electricity materials reported within the literature, including Bi<sub>2</sub>Te<sub>3</sub>, skutterudite, and LAST alloys. The improved numerical model takes into consideration the temperature dependence of the thermoelectric properties of each p-type and n-type materials similarly to total system heat losses. The results show that the highest possible efficiency of the CTG can attain 9,8%, 13,5%, and 14,1% for Bi<sub>2</sub>Te<sub>3</sub>, skutterudite, and LAST alloys, respectively.

Rakesh's [15] paper focuses on calculating the relation between the limiting values of input heat flux for STEG's with Angle of Attack (AOA) and wind direction of the heat sink of the thermoelectric generator. The author investigates the limiting input heat flux for the thermoelectric generator with the hot side at 150 °C. A Computational Fluid Dynamics (CFD) was simulated to validate results with experimental results of Date

[16]. CFD model consists of four TEGs enclosed within a target block and a finned block, in the low-speed wind tunnel. The wind tunnel conditions were maintained according to the outdoor wind conditions. A concentrated solar flux was applied to the target block. From 15°, 30°, 45°, 60°, and 75° AOAs were simulated in the CFD model, and it was concluded that the wind velocities for 4 m/s, 3 m/s, 2 m/s, and 1 m/s respectively, has a very small effect on the Nusselt number ratio for all angle of attack. The ambient temperature when decreased from 16 °C to 11 °C the limiting heat flux increases up to 4,03%. Limiting heat flux decreases, with the increment in ambient temperature from 16 °C to 35 °C, by 13,90%. The study also concludes that the heat sink configuration would affect the value of limiting input heat flux.

The thesis of Bitul [17], investigates the performance of a solar concentrator tube, which is part of the solar trough and is embedded with TEG. The design is indigenous, as the TEG is around the concentrator tube in a curved shape, and the hot side of the TEG is exposed to the solar radiation coming through the glass which surrounds the whole tube assembly creating a temperature required for TEG energy generation. The cold side of the TEG is in contact with the outer surface of the concentrator tube and a heat transfer fluid runs through it to absorb from the cold side. Initially, the design seemed to be very promising but due to the reason the hot side was getting too hot that heat was transferred to the cold side within the tube. This lowered the temperature gradient across the hot and cold side of the TEG assembly and was the only purpose of the design drawback. A completely new concept has been reviewed in the research of Lin [18], in which not only the thermoelectric cooler (TEC) has been introduced but a combination of thermoelectric generator (TEG) and thermoelectric cooler has also been studied. Self-driven thermoelectric cooler-thermoelectric generator (TEC-TEG) systems recently have significant attention among researchers.

The design was created to reduce the convection loss to the ambient by enveloping the concentrator tube. To reduce the radiation loss, the hot side of TEG is covered by a special paint that reduces emissivity and increases absorption. The study emphasis on the following losses (i) Radiation from the absorber surface to the glass envelope (ii) Radiation from the glass envelope to the sky, and (iii) Convection losses from the glass envelope to the ambient air in the presence of wind. A CFD model based on equations was simulated in a MATLAB environment to calculate the temperatures along the concentrator tube.

In the research of the N.Sendhil Kumar [19], it has been investigated that how natural convection occurs in different configurations and instalments. A solar cavity is studied

in the research at  $0^\circ$  and  $90^\circ$  angles for the natural convection. The research also shows results for the cavity with insulation and without insulation. Maximum heat convection while the cavity is covered with insulation at  $0^\circ$  and  $90^\circ$  angles are 63% and 12,5% respectively. The heat convection when cavity is not covered with insulation at  $0^\circ$  and  $90^\circ$  angles are 42,8% and 24,9% respectively. These results clearly shows that the convection has the inverse relation with the inclination angles. The more is the inclination angle the lesser the convection is.

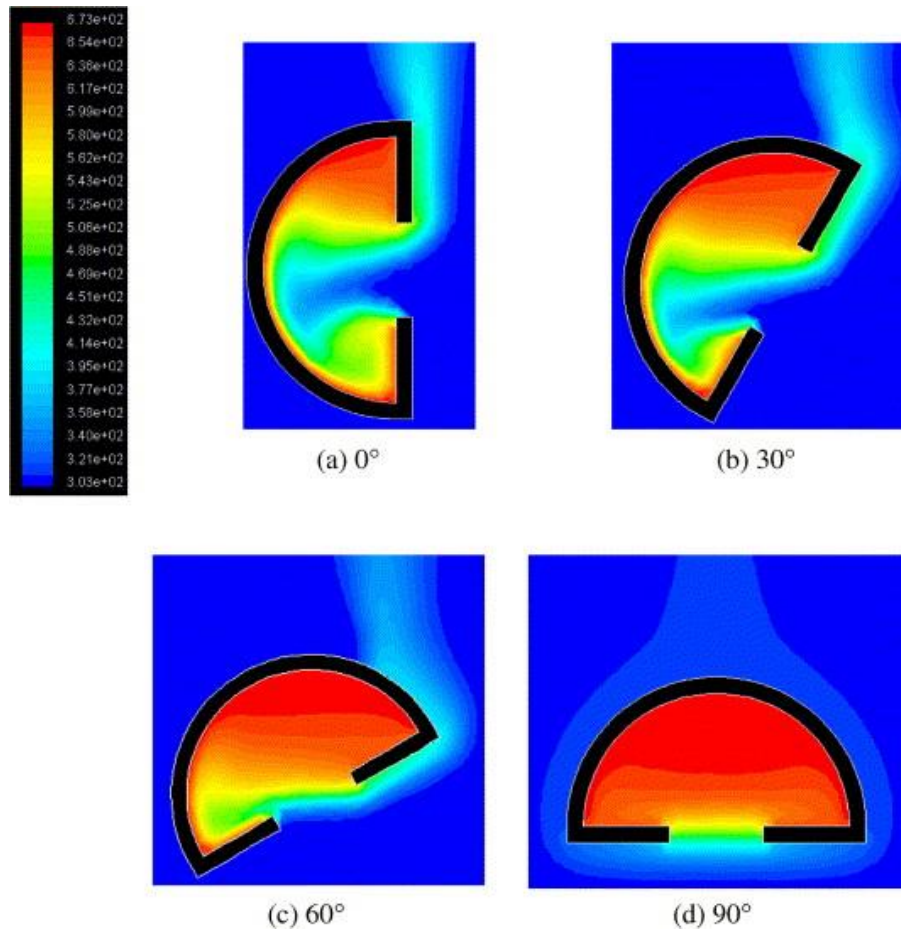


Figure 2.2 Different orientation of solar cavity [19]

## 2.2 Conclusion

In the above literature, it has been reviewed that there has been few limitations and those limitations open an opportunity for me to work on them and optimize the design of a TEG assembly.

- One of the researches is done via Taguchi method only, which is considered useful among researchers, but it has some drawbacks as well. The drawbacks of

this method include use of fractional factorial method that incorporates the minimum number of experimental trials of the received data.

- Only Opto-thermal analysis has been done theoretically and showed that 5% or higher system efficiency can be obtained with or without optical concentration. The analysis has been done theoretically and avoids the thermal leakage between the hot and cold side of the TEG and into the atmosphere.
- The design which has covered TEG assembly in a spherical shaped casing has the drawback that it does not focus on the low-temperature side of the TEG assembly. If design optimization on the cold side of the assembly is considered, the temperature gradient could be higher resulting in increased efficiency.
- The instantaneous thermal efficiency of the dish with cover is lower than without cover which is due to the high convective and radiative heat losses with an increase in the temperature.
- One of the analysis studies considers the value of heat transfer coefficient  $h$  to be infinite which is practically not possible.
- Although the cylindrical design looks very promising the output was not satisfactory. As much as the length increased, the temperature gradient decreased which on the other hand decreased the efficiency.

## **2.3 Objective of the Thesis**

In this research work, the following are the points that will be improved:

- One of the high-priority tasks is to develop a design in which the heat transfer from the high-temperature side to the low-temperature side is minimized, which in turn increases the efficiency of the TEG assembly.
- The heat energy which is being entered into the assembly should not be lost through conduction, convection, and radiation.
- Finding a material, and orientation that is being attached to the hot side of the TEG absorbs the maximum heat energy.
- Selecting the most appropriate material (ceramics) for insulation of heat leakage from hot to cold side of the TEG.
- In real application of the assembly, it will not stay in 90° angle but it will change its angles with the time in a day. Tests will be performed at different angles for the heat transfer.





### 3 CONCEPTS OF HEAT TRANSFER

The science of heat transfer deals with the flow of thermal energy due to the difference in the temperature from point A to point B. In the absence of an external assistance, the heat energy will always move from a hot point to a cold point which is also a conclusion of the second law of thermodynamics. Heat transfer will always occur from hot side to the cold side. We all have experienced that the cup of icy cold water on the table in the room warms up and a warm can of cold drink in the refrigerator cools down. In some engineering problems, heat transfer through the enclosed domain is considered beneficial, for instance, heat transfer through electronic devices via heat sinks but on the other hand, in the electric furnace heat transfer is considered as a downside of a furnace. So, heat transfer depends on problem to problem. This happens due to the phenomenon of heat transfer. Heat transfer occurs in three different ways.

1. Conduction
2. Convection
3. Radiation

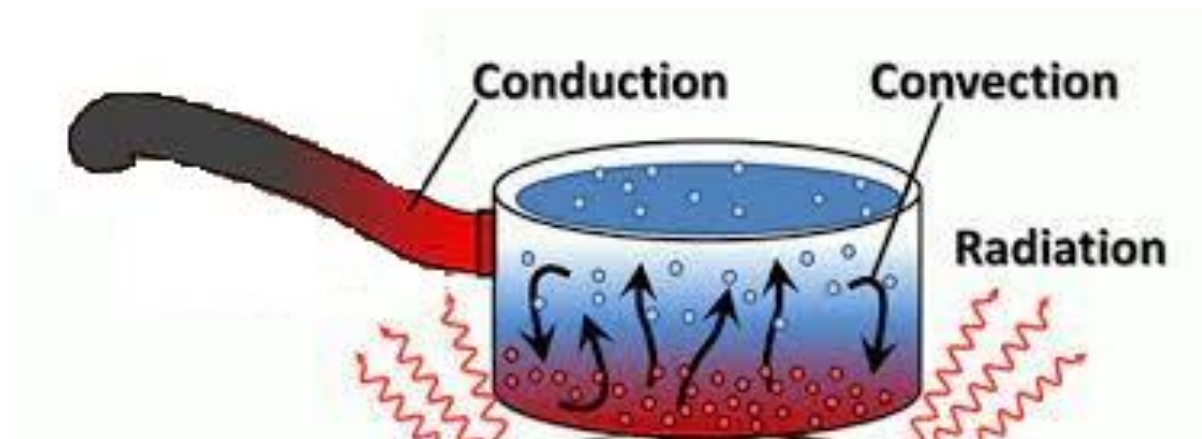


Figure 3.1 Conduction, convection, and radiation illustration [20]

#### 3.1 Conduction

Thermal conductivity is defined as the exchange of heat energy in between the molecules and electrons which are touched together in the conducting medium. The heat flow rate through two ends of a rod material is directly proportional to the area of the rod and to the difference in the temperature between those two ends. Thermal conductivity is inversely proportional to the length. The phenomenon of conduction can occur only in solids. Thermal conductivity is also dependent on the material through

which heat flow. For example, metals have high thermal conductivity than ceramics and glass.

$$Q_{cond} = -kA \frac{dT}{dx} \quad (3.1)$$

where  $Q_{cond}$  – heat transfer through conduction, W,

K -thermal conductivity, W/ (m·K),

A -area, m<sup>2</sup>,

dT -temperature difference, °C,

dx -thickness, m.

## 3.2 Convection

The phenomenon of thermal convection is due to the mass motion of the fluid such as air. Heat or thermal convection occurs from the surface of the object which is being heated which in turns heats up the surrounding air. This heated surrounding air moves away from the heated surface while carrying thermal energy with it. Nowadays, the use of convection has a huge significance, for example thermal convection is used in car radiators to heat sink in electronics devices. There are two main types of convection.

1. Natural convection.
2. Forced convection.

Natural convection is also known as free convection. It is a mechanism or type of heat transfer in which the fluid moves due to the difference in the fluid's density around the heated object. This change in the fluid's density is due to the temperature difference. No external sources, such as fan, suction device or pump is used for the convection. Even the air in the natural convection around the heated part is stagnant.

Forced convection is the type of convection in which external power is required to move the fluid around the hot object. The forcing of the fluid can be done with the help of a pumps, fans etc. To understand forced convection from our daily life, let's consider a hot dinner on a dining table. Before eating hot meal, we blow air on our food, this is a real time example of a forced convection from our daily lives.

$$Q_{conv} = hA(T_s - T_\infty) \quad (3.2)$$

where  $Q_{conv}$  -heat transfer through convection, W,  
 $h$  -convection heat transfer coefficient, W / (m<sup>2</sup>·K)  
 $T_s$  -Temperature of the surface, °C,  
 $T_\infty$  -Temperature of the fluid around the surface, °C.

### 3.3 Radiation

Thermal radiation is a part of three main mechanisms of heat transfer through which bodies exchange heat energy with varying temperature. This phenomenon is specified by the emission of electromagnetic waves from the hot object. The radiation spectrum can range from the ultraviolet to far field infrared light. Thermal radiation is associated with the molecular structure of the receiver, transmitter, and the medium between them. One of the main postulates that differentiate radiation among other sources of heat transfer is that it travels through space as well. The daily life example of radiation can be the heat energy from sun which reaches the earth. The ultraviolet radiation from sun passes through space and hits the earth only through radiation.

The radiation is dependent on the temperature of the emitting object.

$$Q_{rad} = e\sigma A(T_2^4 - T_1^4) \quad (3.3)$$

where  $Q_{rad}$ - heat transfer through radiation, W,  
 $e$  -emissivity,  
 $\sigma$  -Stefan Boltzmann constant,  $5,67 \cdot 10^{-8}$  W / (m<sup>2</sup>·K<sup>4</sup>),  
 $A$  -area, m<sup>2</sup>,  
 $T_2$  -surface temperature, K,  
 $T_1$  -ambient temperature, K.

### 3.4 Validation with the empirical solution

Initially, the validation of the model simulation work is done on a 6x6x1 cm insulation flat plate. The value of conduction through the insulating material is calculated analytically and then that result was compared with the simulation results using ANSYS. The material properties of the insulation material, also used as main insulation material of the system are given in Table 3.1 below:

Table 3.1 Mechanical properties of the Skamotec material

Properties		Units	Values
Bulk density		kg/m <sup>3</sup>	225
Total porosity		%	91
Specific heat		kJ/ (kg. K)	0,84
Thermal conductivity	10°C	W/ (m·K)	0,061
Thermal conductivity	200°C	W/ (m·K)	0,07

Table 3.2 Chemical composition of Skamotec insulating material.

Chemical analysis	Composition	%
Silica	SiO <sub>2</sub>	47
Alumina	Al <sub>2</sub> O <sub>3</sub>	0,2
Ferric oxide	Fe <sub>2</sub> O <sub>3</sub>	0,1
Magnesium oxide	MgO	0,4
Calcium oxide	CaO	42
Sodium oxide	Na <sub>2</sub> O	0,1
Potassium oxide	K <sub>2</sub> O	0,1
Loss on ignition at 1025°C (1877°F)	LOI	9

Considering a piece of material having thickness of 1 cm (0,01 m) and side area of 0,0001 m<sup>2</sup>, a comparison of the calculation of heat conduction is presented.

ANSYS model uses 3D model of the material piece, subjected to hot side temperature of and all the other similar boundary conditions were applied.

The results calculated with simple analytical expression are almost equal to the results of the simulations. The methodology to calculate conduction in a flat plate is that it has provided a temperature of 215°C and the temperature on the other side of the plate is at 25°C. The calculated conduction is 4,78 watts and the value obtained through the simulation is 4,17 watts. Same boundary condition is applied to the simulation as to the boundary conditions were considered while solving this problem empirically.

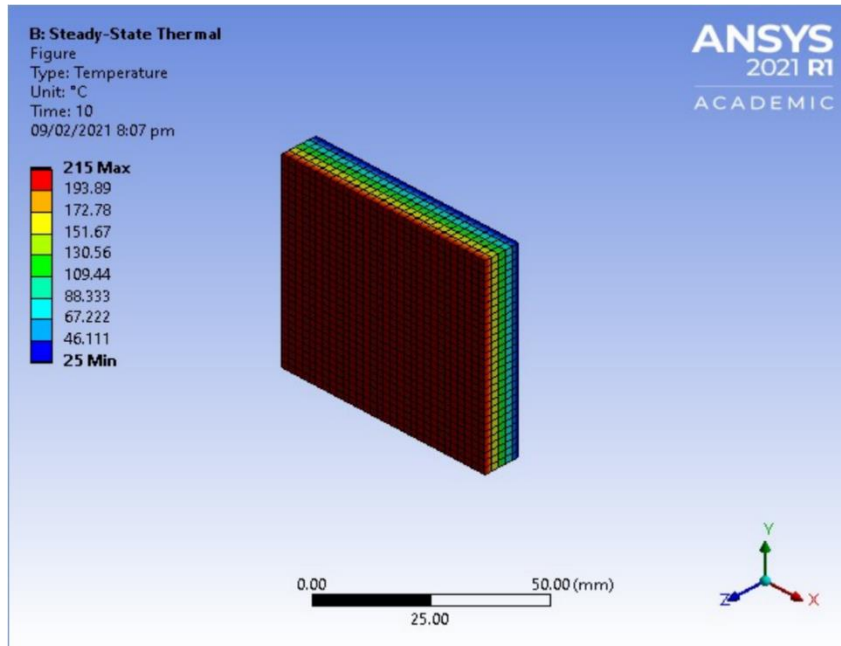


Figure 3.2 The temperature gradient across the plate

$$R_{\text{Insulation}} = L / (k \cdot A) \quad (3.4)$$

$$\dot{Q}_{\text{Insulation}} = \Delta T / R_{\text{Insulation}} \quad (3.5)$$

$$\dot{Q}_{\text{Insulation}} = \frac{(T_{\text{hot}} - T_{\text{cold}})L}{k \cdot A} \quad (3.6)$$

where L - thickness of the insulation = 0,01 m,

K- thermal conductivity,

A -area of the plate,

$\Delta T$  - change in temperature = 190°C,

$R_{\text{Insulation}}$  - thermal resistance = 39,7 K/W,

$\dot{Q}_{\text{Insulation}}$  - total conduction through the insulation material, 4,78W.

### 3.5 Methodology

The finite element method (FEM) or finite element analysis (FEA) is the simulation technique that is used so widely that it covers the solution of every engineering and mathematical model. To solve any real-life example, FEM is used, and it subdivides the large systems into smaller and simpler parts that are named as finite elements. FEM is a method of mathematically modelling the stresses on a considered engineering design. The considered engineering design can be of structural analysis for calculating stresses and strains, fluid dynamics for calculating or observing the fluid's behaviour, and heat

transfer for measuring and observing thermal stresses and heat transferred on the design.

The reason for so widely use of FEM is that it gives you an opportunity to optimize your product design efficiently without manufacturing or building the real product or prototype. By applying this method, risks of inappropriate wear and damages can be minimized. One of the substantial significances of FEM is that it is very cost-efficient because critical areas on the design can be recognized before manufacturing the real product. Using this method in the design phase, the selection of optimized material can also be done by considering material properties. To summarize the essence of FEM, it is the finest possible way of design phase so far and cost-efficient. According to the society of automotive engineers (SAE), when FEM is used properly, it becomes a tremendous productivity tool and helps design engineers to minimize product development time and cost as well at the same time.

In this master's thesis research, the focus will be on the finite element method for the optimized design of TEG assembly and by using manufacturing processes, prototype will be fabricated of a proposed design. After manufacturing the prototype, physical tests will be performed on that assembly by applying heat and measuring the temperature on different surfaces of the prototype. With the help of the finite element method, the selection of the best insulating material will also be simulated and will be applied to the manufactured and finalized design of the TEG assembly. Initially, the proposed design will be visualized to a 3D model using Solidworks and alterations will also be made in the same 3D model to optimize the whole design. The 3D model will also be made in consideration of available additive manufacturing technologies in our university. For thermal analysis of the design, ANSYS is one of the most used tools among researchers and scientists. ANSYS is well-known due to its up-to-date versions and a wide range of modules, for instance, static structural to explicit dynamics and computational fluid dynamic CFX to thermal analysis.

As far as measuring the success of the research is concerned, the optimized results are the scale for the successful research. The goal is to achieve a design that can offer minimum leakage of heat from the high-temperature side to the low-temperature side. One another study is about the selection of the insulating material which will be used in an efficient way to make the whole TEG assembly work better. The results from FEM cannot be perfect the same as the results or numbers from physically testing the prototype because of the tolerances and computational ideal construction and other assumptions due to the academic version of ANSYS.

For this thesis work, steady state thermal module has been used to simulate a wide range of considered geometries. This module can be used in the academic version of ANSYS with limited number of nodes and elements in the mesh. Apart from the mesh

constraints, some assumptions have also been made due to the version of ANSYS. The figure below shows the steady-state thermal module, geometry module and Engineering data module. Engineering data module carries all the material properties which will be used for the simulation. The geometry module is used to import 3D models which were being designed in Solidworks to ANSYS. Steady-state thermal is used to set up all the boundary conditions, values and get the results. All these three modules are interlinked to each other and share data in Ansys workbench.

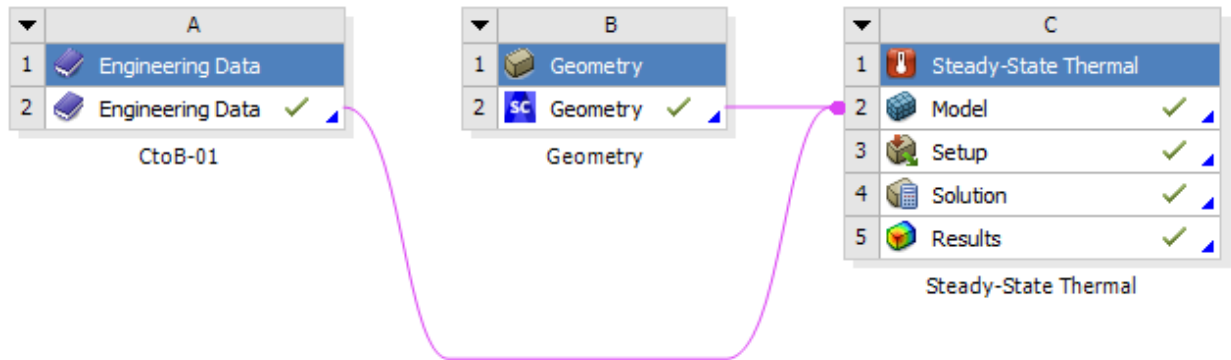


Figure 3.3 Ansys workbench modules

In the figure 3.3 the engineering data represents the material properties which is being considered for the design optimization of the TEG assembly. Most of the material properties which is being used is input into the setup of the engineering data section of Ansys. Every model which is prepared in Solidworks is being converted to the .igs file and imported to the space-claim of Ansys afterwards. Some of the changes in the models are also being made in the space-claim and then linked engineering data and space-claim geometry with the steady-state thermal module. As the figure 3.3 shows a pink line that is going through the engineering data box to the steady-state thermal and space-claim geometry to the steady-state thermal. All the boundary conditions, meshing and solutions are done in the steady-state thermal module.



## 4 ABSORBER'S INSULATION DESIGN

The base design of the solar thermal absorber has been developed through the previous experience and lessons learned. In this thesis the thermal absorber design has been further optimized and analysed to identify the key parameters to provide best efficiency with minimum material amount.

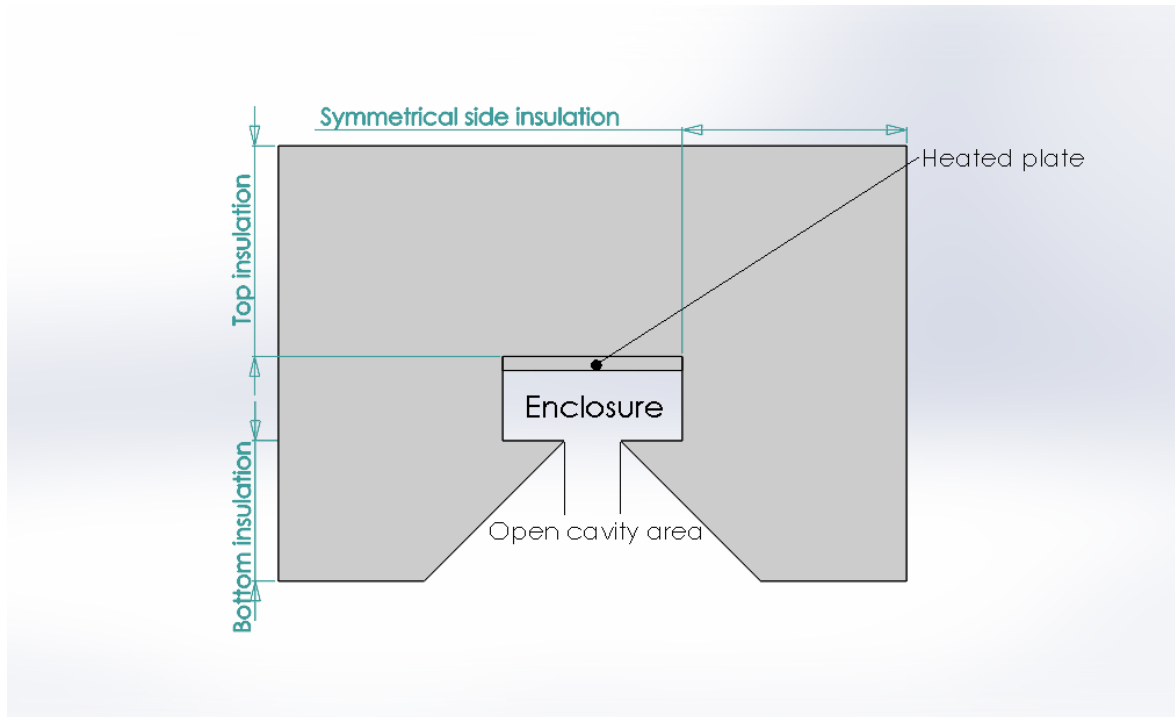


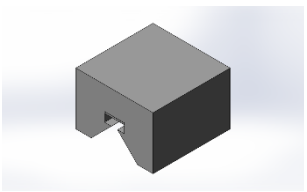
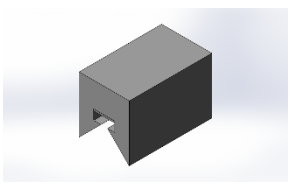
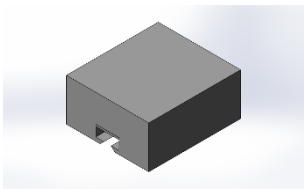
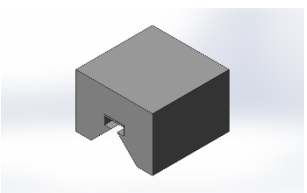
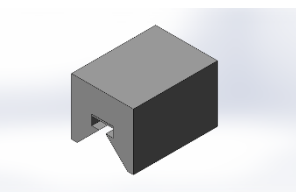
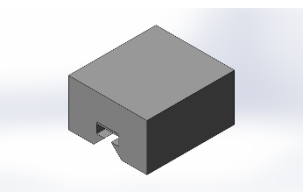
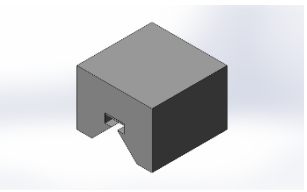
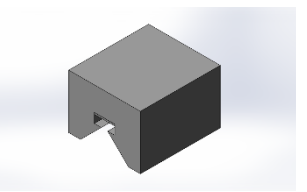
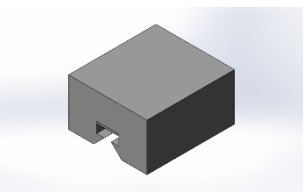
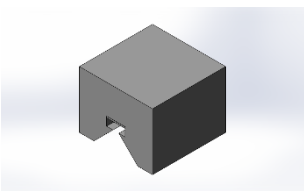
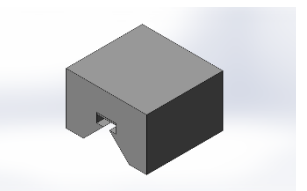
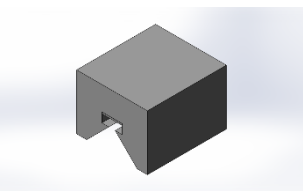
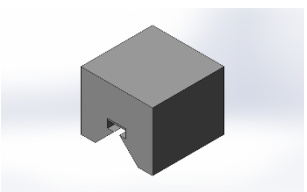
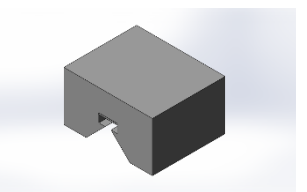
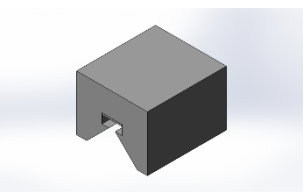
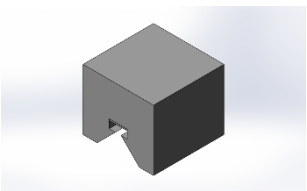
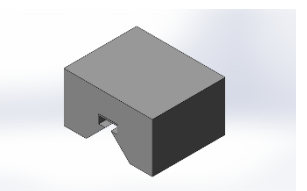
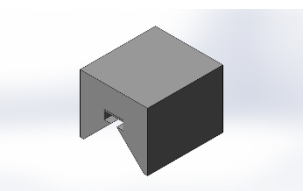
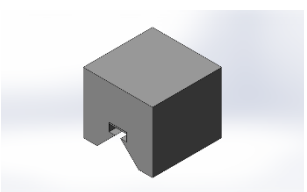
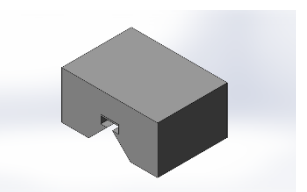
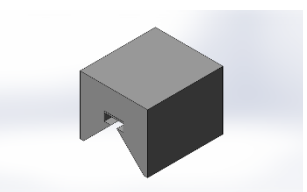
Figure 4.1 Description of absorber's insulation

In the previous research works on the same topic, the model was just fabricated without considering the optimum dimensions and parameters. No model calculations according to any of the three types of heat transfer were measured and compared. In this thesis the work is done which was not considered in the previous research. First of all, 3D models were built and were simulated for the best power output. Afterwards, optimum design was fabricated. At the end of this thesis tests were made at different configurations and orientations of the assembly.

For the development of optimized structure, around 50 designs have been simulated with different dimensions and boundary conditions. The centre to top insulation dimension varies from 30mm to 160mm, centre to left and right dimension varies from 44mm to 140mm and centre to bottom dimension varies 40mm to 120mm.

The absorber's geometrical key design has been developed in Solidworks and been imported to the Ansys interface of space claim. The absorber's geometry is then linked with the steady state thermal module in the Ansys workbench.

Table 4.1 Following models are the sequence of the absorber's geometry which is being modified:

S #	Centre to top	Centre to left & right	Centre to bottom
01			
02			
03			
04			
05			
06			
07			

The geometries provided in the table above are the isometric view of most of the considered geometries. Initially, the dimensions are taken from the work done previously. Then, changes in the dimensions were made and modified design was simulated. In the above table, the first column shows the centre to top dimension in an increasing order. The same way the second column shows the centre to left and right dimension and the third shows the centre to bottom dimension in an ascending order.

## 4.1 Meshing

Meshing is a significant and major component of finite element method and engineering simulation processes. Through meshing, intricate geometries are divided into simpler elements and nodes. Afterwards, those simpler elements are used as discrete local approximations of the bigger domain. The meshing has a great influence and effect convergence, accuracy, and speed of the simulation. In finite element method, due to fine meshing, the results obtained are fine which in turns takes more computational power or time to show results. It means that the finer the meshing is, the more accurate results are, and more computational power will be required. For this thesis, the mesh size, which is allowed and permitted by the Ansys for their academic's version is considered. For all the models, number of nodes are around 17000 and number of elements are around 8000. Mesh refinement on all the surfaces is also applied so that mesh becomes finer.

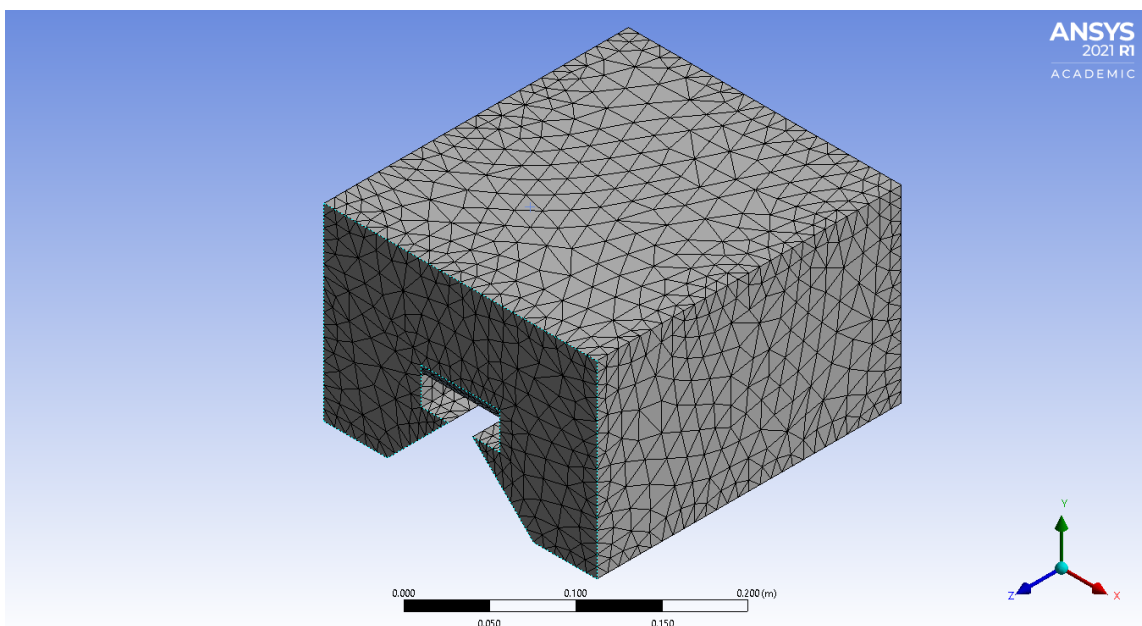


Figure 4.2 Absorber's meshing

Statistics	
<input type="checkbox"/> Nodes	16604
<input type="checkbox"/> Elements	8016

Figure 4.3 Mesh size examples

## 4.2 Different boundary conditions and enclosure

Boundary conditions of the absorber's part has been changed and was simulated in the steady-state thermal module of Ansys with the same mesh size and material details as done while optimizing the geometry by changing its dimensions. The boundary conditions play very important role in the whole simulation, including results. Following are the changes in the boundary conditions:

1. Initial surfaces with hot temperature applied to heated plate.
2. Addition of the convection surfaces.
3. More convection surfaces added.
4. Addition of the radiation of the emissivity value of 0,5.

In addition to radiation, emissivity of the absorber's surfaces was kept 0,5. According to definition of emissivity, the effectiveness of the surface of a material in emitting energy as thermal radiation is called emissivity. It is also a ratio of the radiant energy emitted out of the surface to that which is emitted by a blackbody at the same temperature.

## 4.3 Simulation results

In the figure 4.4 below, the graphs represent the output of three different models, each having different boundary conditions, as described. On the graph, the horizontal axis shows the type and applied boundary condition on the geometry whereas on the vertical axis is the output (W). T1, T2, and T3 are the three types of the absorber's geometry and number next to them indicates the applied boundary condition. For example, T1-01 represent the first geometry in the figure 4.4, having different surfaces of hot temperature applied.

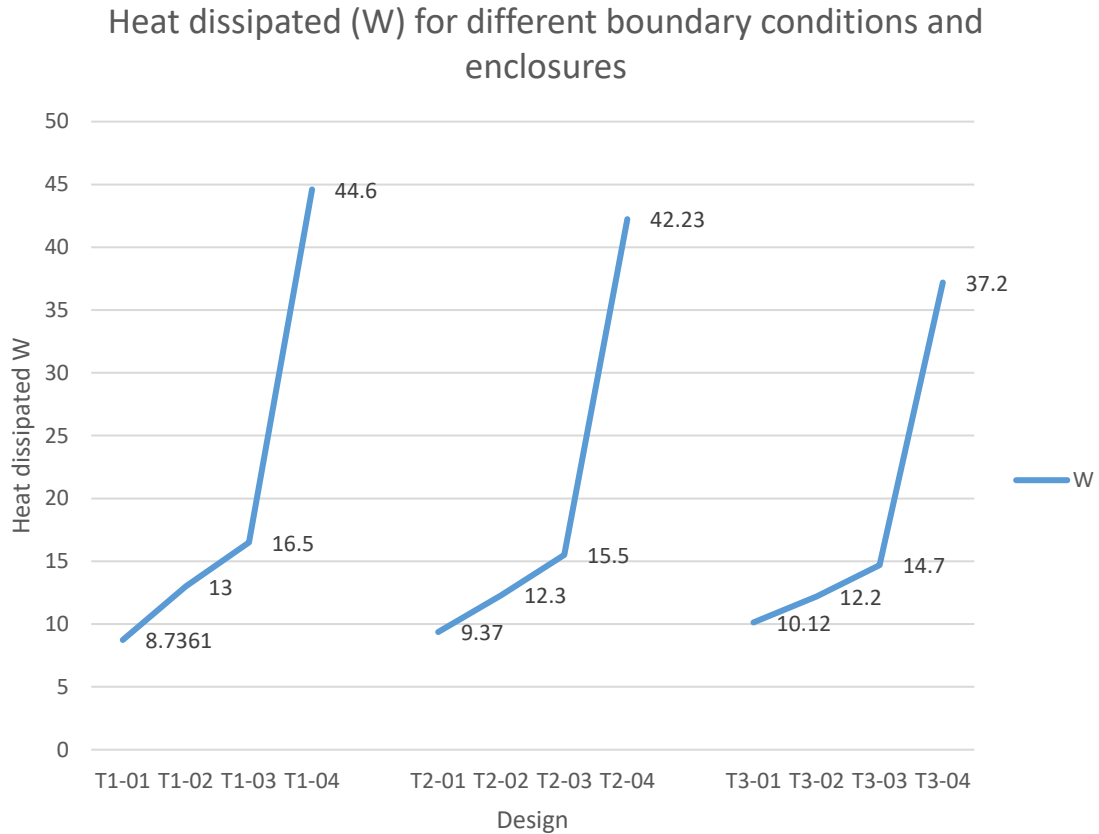


Figure 4.4 Different boundary conditions

The graph above also shows that when the boundary conditions in the Ansys are set to more surfaces which emit heat energy due to conduction, convection, and radiation results in more heat loss. The huge gradient in the values of T1-01 and T1-02 is due to the surfaces emitting heat energy through convection and the small increase in the values of T1-02 and T1-03 is due to the fact that the only two more surfaces were added to heat loss through convection. The escalation after the third point is due to the radiation surfaces added in the geometry in every type. The surfaces which emit radiation were the highest temperature surfaces. In general, if the overall heat loss is concerned then it has been proven with the graph above is that the heat loss decreases with the increase in the length of the enclosure. The first type has zero length of enclosure while the third type has the maximum length. The difference in the maximum heat loss of first type is much higher than the maximum heat loss of the third type. In short, the length of enclosure of the third type is the optimum length.

## 4.4 Base for optimization

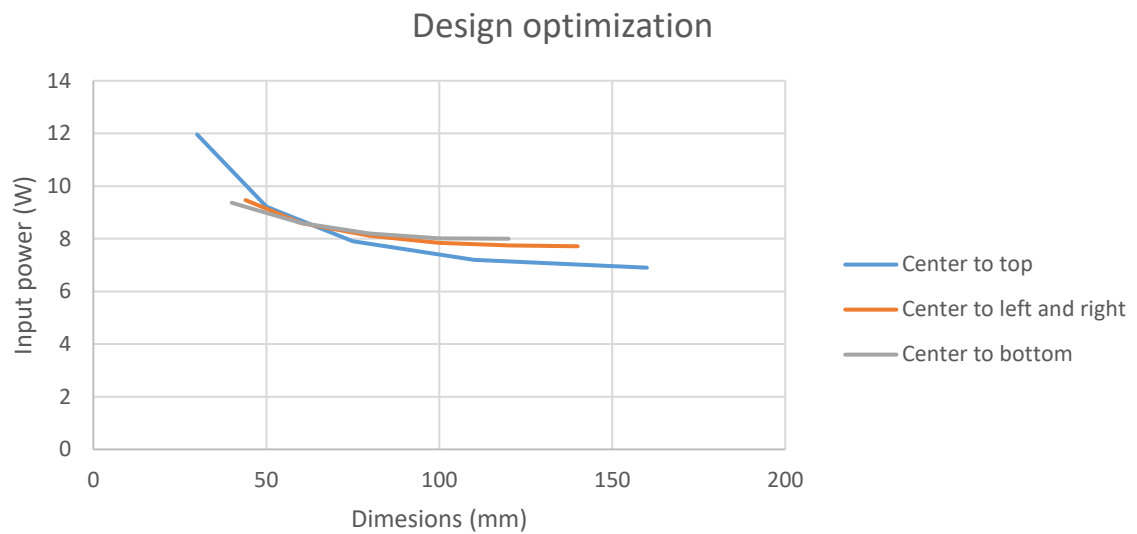


Figure 4.5 Results of thermal losses in different simulated models

The graphs above clearly show the sudden drop in the convection heat loss through the outer surfaces of the geometries. At first, the optimum geometry was chosen while simulating the centre to top alteration in the dimensions, after that centre to left and right alteration in the dimensions was performed and at the end, the most optimum was selected while performing centre to bottom alterations in the dimensions. The criteria for selecting the optimum dimension from the centre was to select a point after which the line in the above given graphs become straight or the gradient as compared to the increase in length of the insulating material becomes less.

After simulating and getting heat loss through convection and conduction, the optimum dimensions of the absorber geometry has been selected. In the table 4.1, the third geometry shown in the centre to bottom column is the most energy saving geometry among all of them. The figure below shows the optimum geometry with the optimum dimensions on it. These dimensions are in mm.

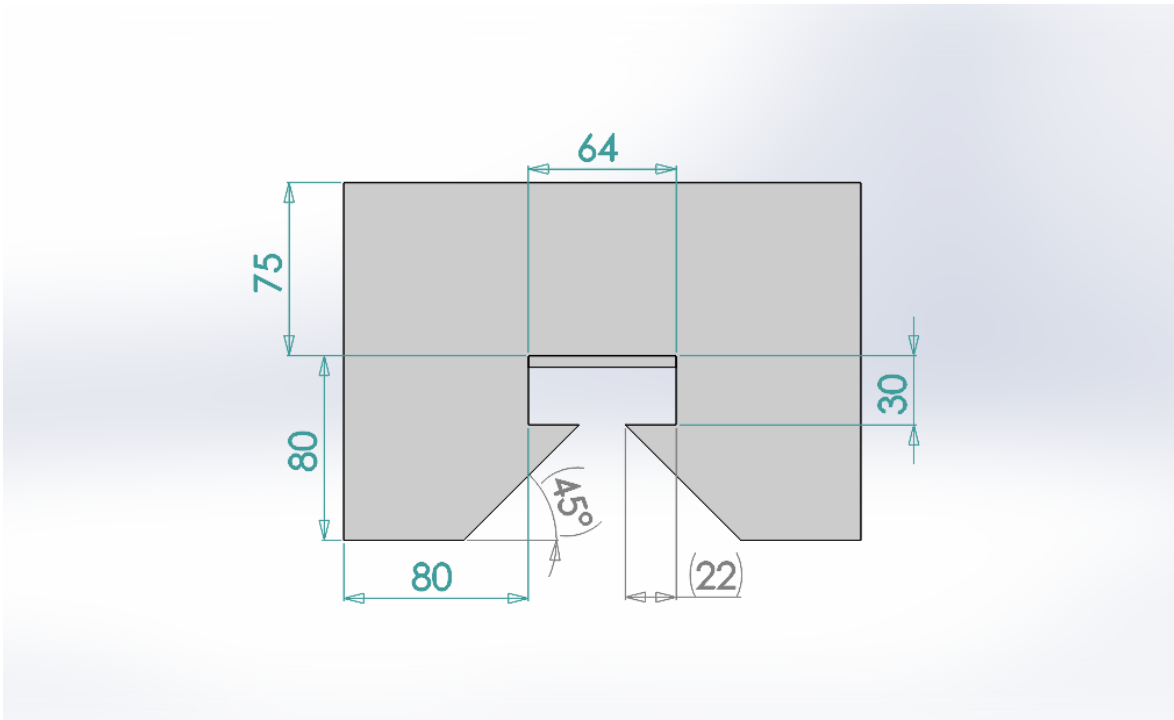


Figure 4.6 Most optimum dimensions

In the table 4.1, all the models were being imported to the space-claim of Ansys and were simulated for temperature distribution and heat loss. The mesh size for all the geometries is same. In the following table 4.2, optimum dimensions are considered for the absorber is given:

Table 4.2 Ansys simulations for design optimization

Centre to top T1	Centre to left and right T2	Centre to bottom T3

The table 4.2 above is the set of optimum geometries which also shows the temperature contours around the hot side of the plate. The area which is in red colour shows the hottest area in the geometry. The pictures in the table 4.2 also shows that the temperature is distributed towards the outer surfaces of the geometry through conduction.

## 5 FABRICATION AND TESTING

The fabrication and testing of the assembly is completed in the workshop at the Tallinn University of Technology. The target is to build and test a reliable heat insulation in a specified geometry. The insulating material is cut according to the geometry from a flat piece of board. The assembly was also fabricated that it could be adjusted easily without disassembling the whole assembly. In addition, the heated plate could also be separated from the whole assembly without separating any of the parts. The design of an adjustable assembly is because it can be used for different orientations and configurations. In a nutshell, the current design of the assembly is the finest from previous assemblies.

### 5.1 Previous and currently used and tested insulating material

In the previous research done on the similar topic. Few experiments on different insulating materials have been done. The insulating material includes refractory foam, stone wool, and ceramic wool. Properties of these materials are given in the table below:

Table 5.1 Properties of previously used insulating materials

Feature	Fire-resistant foam	Stone wool	Ceramic wool	Calcium silicate material
Operating temperature (°C)	321	750	1150	-
Maximum temperature	600	-	1260	-
Thermal conductivity (W/m-K)	0,034	0,035	0,12	0,061
Density (Kg/m <sup>3</sup> )	15-30 (Depending on size)	100	128	225
Shape	Balloon	tile	roles	flat rectangular boards

#### 5.1.1 Fire-resistant foam

In the previous research work, fire-resistant foam was tested as an insulating material. EN1366-4 and DIN4102-1 compliant fire-resistant foam, which is also rated as foam B1, did not work. The previous research says that although it is suitable for the operating



temperature of 321 °C, but it has been tested that in a suitable ambience, even at 300°C, this fire-resistant foam melts and emit gases.

### **5.1.2 Stone wool**

This insulating material was tested and even once used in the same conditions for the research previously. As mentioned in the properties of this material it can withstand the temperature of 750°C. Unfortunately, this insulating material also did not work for this certain temperature. Stone wool at the high temperature ranges started to emit gases. It is stated in the previous research work that the colour of the stone wool also changed at the temperature of 363°C.

### **5.1.3 Ceramic fibre wool**

In the latest research, which was being carried out so far, used ceramic fibre wool. This material was initially tested and proved that it does not change colour, shape and emit gases. In short, this material seemed to be the perfect insulating material. All though this material fits for all the constraints and problems which were occurring in the previous tested materials, but it also had some different problems and constraints. The first obstacle in using this material is that it releases some harmful particles if inhaled. So, handling this material was an issue. Strict safety measures were to be taken for using this material in the TEG assembly.

To keep this material intact was another challenge to use this material in this assembly. As this material is like cotton wool, a perfect assembly was required to forcefully keep this material intact and in place so that it operates and works in the same manner as expected. The following picture shows the test being conducted on the ceramic wool at higher temperature ranges:

### **5.1.4 Currently used calcium silicate material**

In this thesis work, calcium silicate material Skamotec, is used for the insulation purpose. These rectangular boards were easily cut to the desired shape with the help of a saw in the workshop. After cutting the large flat boards to the desired shape, the pieces were glued together with the help of specialized enclosure glue. Heat endurant

enclosure glue works with the calcium silicate material to keep pieces together. This material is usually used for covering the furnaces which are at high temperatures.

## 5.2 Heat source part

The core of the whole assembly is the heated plate simulating for solar absorber. Heated plate consists of five resistance heaters and four temperature sensors. To obtain the accurate measurements from the sensors, the sensors should be strongly attached to the heated plate. Ceramic material was used to hold the sensors at four different locations on the heated plate and in a specific configuration. Ceramic was only used because it is easy to machine, and it is heat resistant. Heated plate was fabricated with much care because of the complexity of complex circuit on it.

The circuit of the heated plate was designed while considering making it as much robust and reliable as possible. The whole circuit is complex to hold because at this temperature, printed circuit boards cannot be used. Few parts were also manufactured with stainless steel in the workshop. Resistance heaters were placed side by side, attached to each other so that a single wire could be used for the single terminal of all the heaters and other wire for the other terminal. These connecting wires are designed not only for the electrical connections, but they are also used to hold all the heaters in one place. As shown in the picture below, wire is wrapped around the stainless-steel rectangular plate for the connection and holding the heaters. The wires are wrapped around the plate because they also provide a cushioning effect to hold the heater.

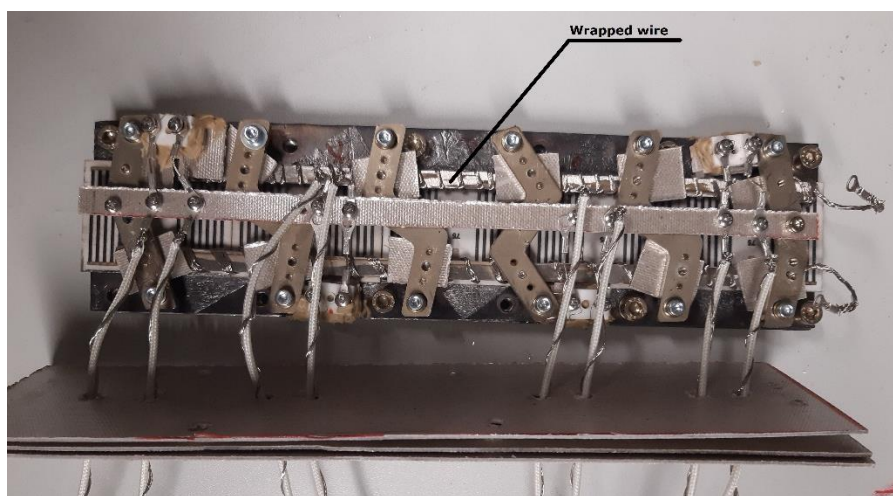


Figure 5.1 Heated plate

The figure below shows the circuit of the heated plate. The sensors have two terminals which in turns to four terminals. Two terminals for voltage and the rest two for the current measurement. Two bars for the heater's connection through the heated plate also helps to hold the resistance heater in the circuit. Direct current is provided to the heaters of the heated plate. Total resistance of the heaters is ohms.

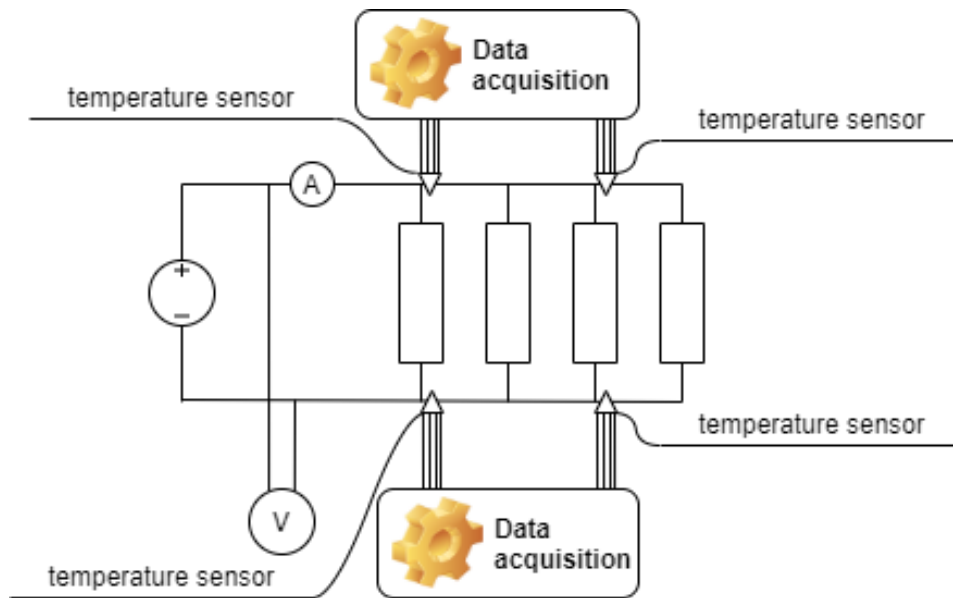


Figure 5.2 Heated plate circuit

### 5.3 Temperature sensors

PT1000 temperature sensors are the most sensitive device in the whole assembly. These sensors are tiny and can sense temperature gradient on a very small scale. This 3,5 x 2 x 1 mm device holds a state-of-the-art technology in them. Two terminals emerging out of minuscule piece which itself is a pair of two part. These two parts are configured on the heated plate in a way that the white side should always touch the heated plate and the blue part is on the other side. The two terminals coming out of blue and white parts are then connected to the data acquisition unit. From data acquisition unit measurements were shown and recorded in the computer. The figure below shows two temperature sensors.

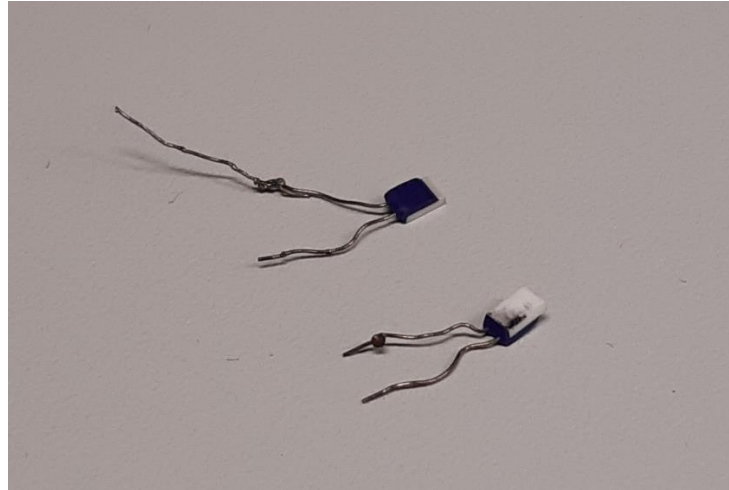


Figure 5.3 Temperature sensors

## 5.4 Fabrication of a robust assembly

In order to make a robust design of the assembly, several alterations were made to fabricate a robust design. One of the main tasks in the fabrication of the assembly is that every part should be firmly attached to the outer structure, which is made of eight L-profiles. Four of the L-profiles are little longer because of the screws going through them to attach the upper structure with the lower structure. In between the structure of the L-profiles, there are insulating material pieces with the heated plate, exactly in the centre.

Whole assembly is joined together with the help of aluminium L-profiles as an outer structure and M3 bolts. The upper and lower structure is also fastened together with M5 threadscrew. The assembly consists of following parts:

1. Insulating material
2. 4x4 L-profile
3. Glass wool
4. Sensors
5. Ceramic heaters
6. Small ceramic insulators
7. Nuts and bolts

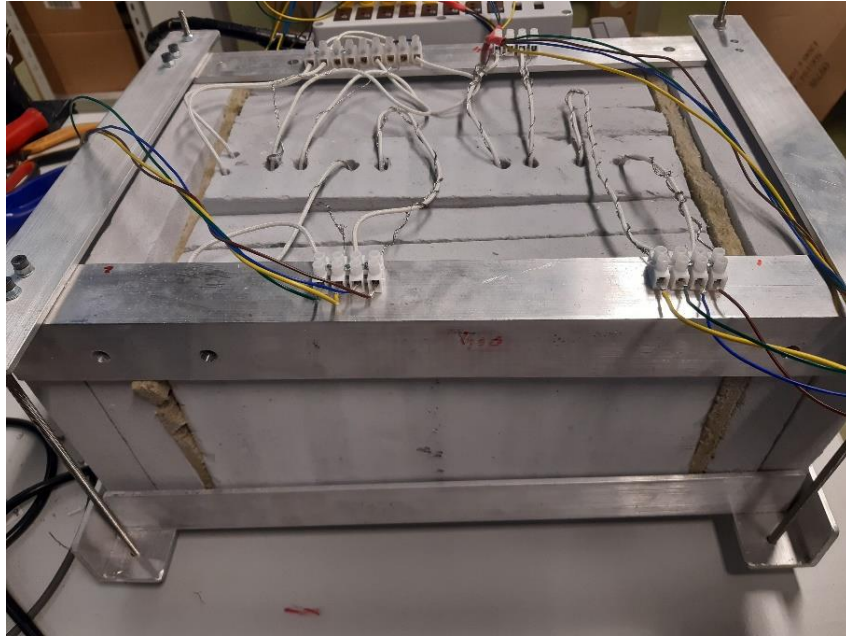


Figure 5.4 Fabricated assembly

### **5.4.1 More robust and adjustable alterations**

The design of the outer frame is keeping all the parts intact in one assembly. The design quality of the outer frame of the assembly was acceptable but due to the requirement to adjust the whole assembly again this current frame design was little rigid and did not has a flexibility to adjust. To make it more adjustable, few alterations were made, like the use of threaded studs and two plates with holes to make the adjustable assembly strongly intact. The threaded stud allows to tighten the parts as much as possible. Below is the final outer frame which is more adjustable and keeps all the parts more intact.

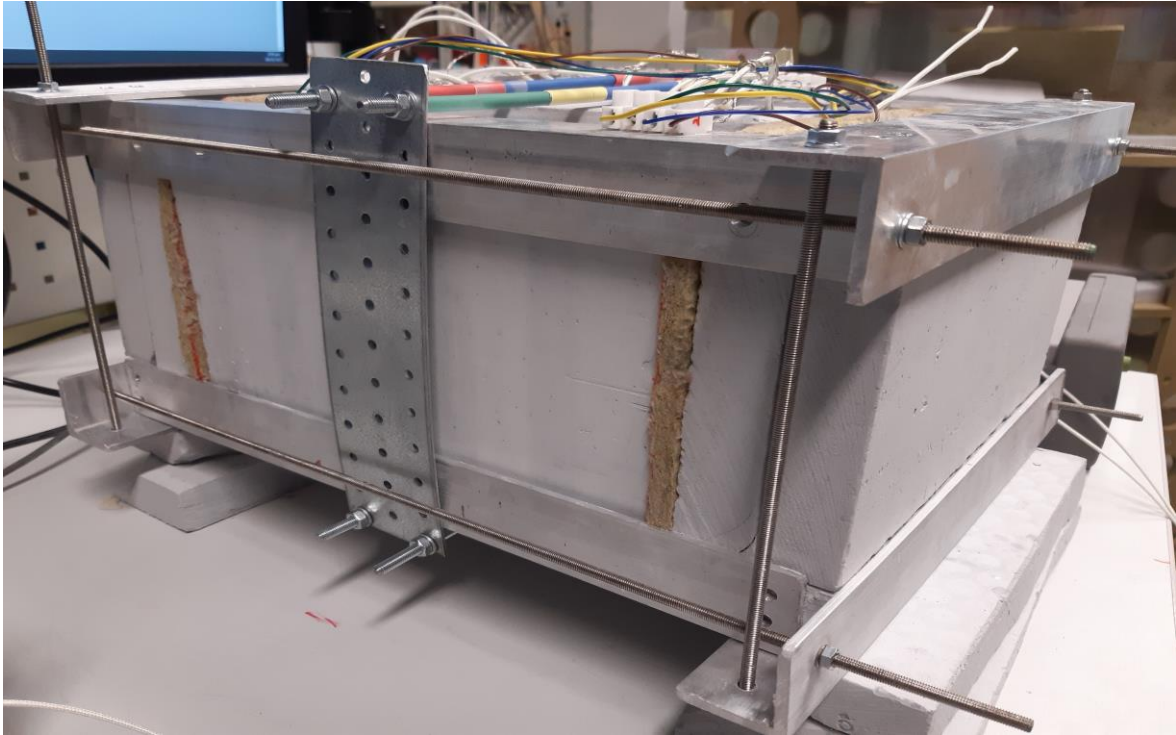


Figure 5.5 More adjustable outer frame

## 5.5 Power supply

BK Precision 9130B triple output programmable DC power supply was used to input the desired voltage, current and power to the resistant heaters inside on the heated plate. The testing was done on different values of power. This power supply has three channels because it allows to supply different power outputs at the same time. Only the first channels are used to heat up the heated plate through resistance heaters.

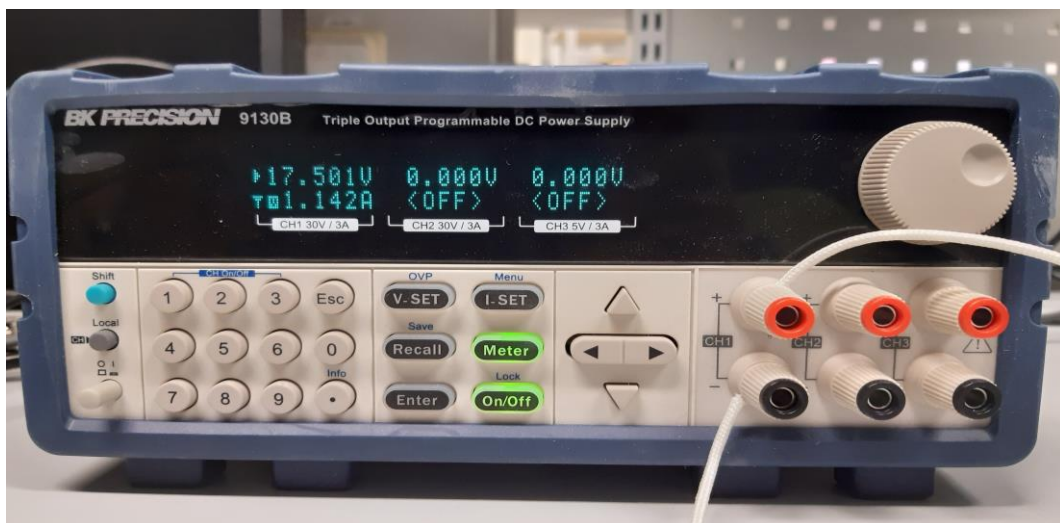


Figure 5.6 Power supply

The software interface of the BK Precision power supply is interactive. All three channels are given in the initial interface of the software. After specifying the voltage and making all the connections to the output of the power supply, the software automatically calculates the output power. To setup the software, the installation files were downloaded from the internet and were being installed in the computer. After installation, connections were made. This power supply converts 230V AC to the desired DC voltages. At the end, the device was configured with the software. The software also has three knobs to change the voltage and three knobs for the current. The user can also type the desired values of voltage and current.



Figure 5.7 Power supply user interface

## 5.6 Data acquisition software and device

Keysight 34972A data acquisition / switch unit device is used for the compilation of the data from the temperature sensors and the input power. This device is integrated with the Benchlink data logger software in the computer and is connected through a USB cable. 20 slots are available with this device to connect sensors for data acquisition. A small LCD is also in place for the display.



Figure 5.8 Keysight data acquisition device

Keysight data acquisition device is linked to the benchlink data logger software via USB cable. This software was installed through a CD available with the device. Before installing the software, I/O libraries were installed from NI Visa libraries. After installing the software, the instrument was configured in the software.

The next step after the device configuration, was the configuration of the scan lists, which means that which terminal contains which sensor and which terminal measure which parameters. After setting few other parameters in the software, quick graph tab is used to observe the graph after pressing the play button in the menu bar of the software.

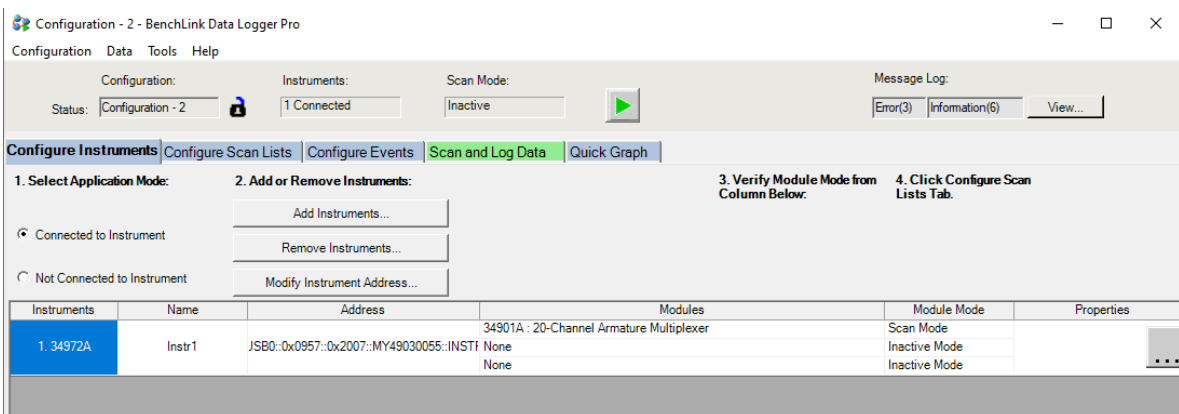


Figure 5.9 BenchLink data logger

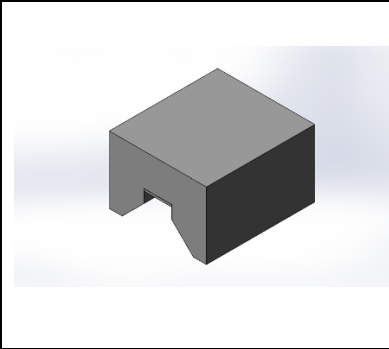
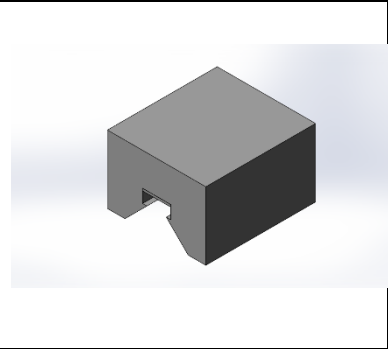
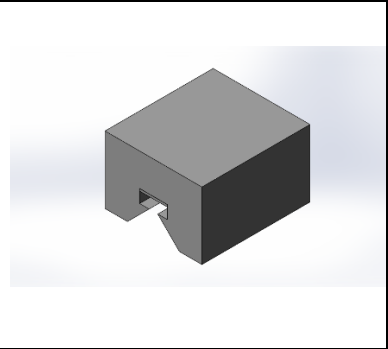


# 6 TESTING

## 6.1 Comparison base for testing

Different boundary conditions were applied to three different types of the absorber's geometry. The manipulation in the absorber's design was done in the centre or to the open cavity of the enclosure. The size of the barriers of the enclosure were changes and were being simulated to get the outputs. The same enclosure sizes were also tested of the prototype in the laboratory.

Table 6.1 Different boundary conditions on different enclosures:

Type 1	Type 2	Type 3
		

Different geometries have been observed during the testing. This way a piecewise approach can be taken to compare the actual thermal cavity performance to Ansys model. It is expected, that the Ansys model could only partially describe the cavity radiative losses.

Testing and parameter investigation started with gap fully open. Radiative losses would correspond to absorber part black body radiation. This is the least approach model for analysis. Next, identify true conductivity, then true emissivity, then actual convection results. Then, close the gap a bit, assume conductivity is the same as first tests, find radiative losses levels, after that observe convective losses. Last, gap at initially proposed width, steps as in prior stage.

## 6.1 Thermal leakage and build quality

Thermal tests and readings were also taken in parallel from the outer assembly to check which part of the assembly is dissipating heat the most. For this purpose, FLIR thermal camera was used to measure the surface temperature.

In the picture below, the contour shows different meaningful colours. The red and white colour shows that this part of the surface is the hottest and the blue colour means that this area has the minimum surface temperature. With the help of this thermal camera, the average temperature of the surface which is being covered by the camera is also calculated. The value of the average temperature of the surface is shown on the top left corners of the pictures.

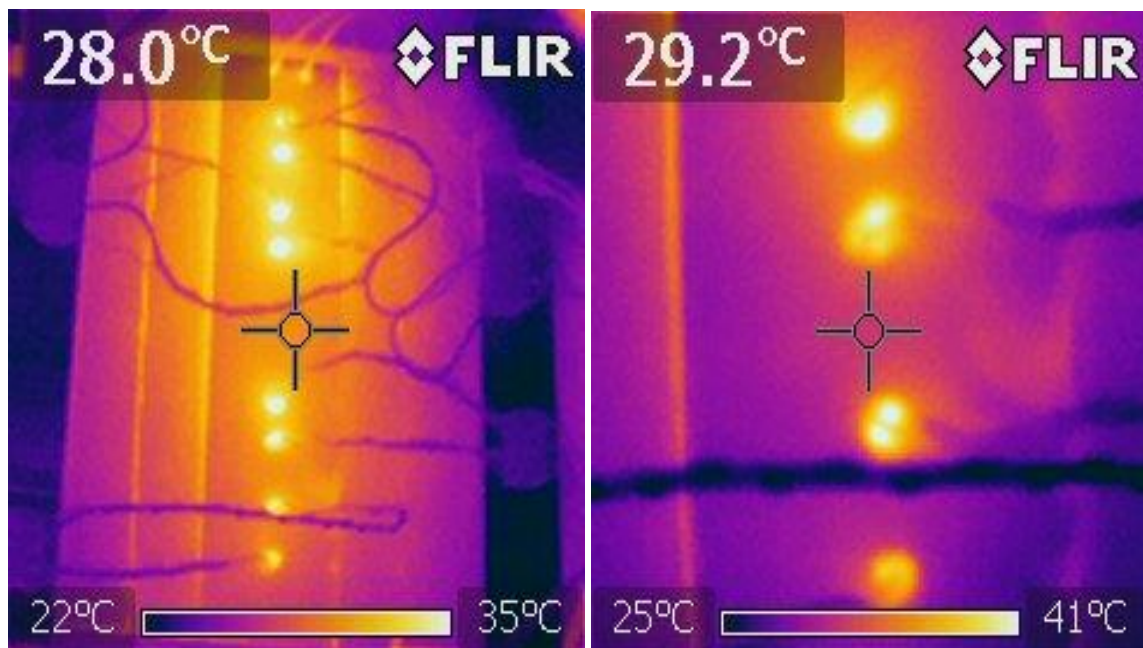


Figure 6.1 Thermal camera contours

## 6.2 Testing of fully covered assembly

Several tests were made, and temperatures were recorded with the help of temperature sensors. At different power inputs, temperature sensors were measuring different values. It has been observed that for more power input, the temperature sensors were measuring more values and vice versa. The table below shows different temperature output against different power inputs.

Table 6.2 Power against temperature, fully closed insulation enclosure

First Assembly		
S. No	Power input (W)	T (°C)
1.	10	111
2.	20	180
3.	30	235
4.	40	293

Some alterations were made in the outer frame of the assembly and then tests were made. The iterations are already discussed in the topic (5.4.1). The results obtained after making the outer frame adjustable are given in the table below.

Table 6.3 Second and third assembly, fully closed insulation enclosure

Second Assembly		
S. No	Power input (W)	T (°C)
1.	10	103
2.	20	186
3.	30	238
4.	40	308
Third assembly		
1.	20	192
2.	40	320

In the tables 6.3, it has been clearly illustrated that the more adjustments and iterations made in the assembly or the better the assembly gets, the better results and temperature values are obtained.

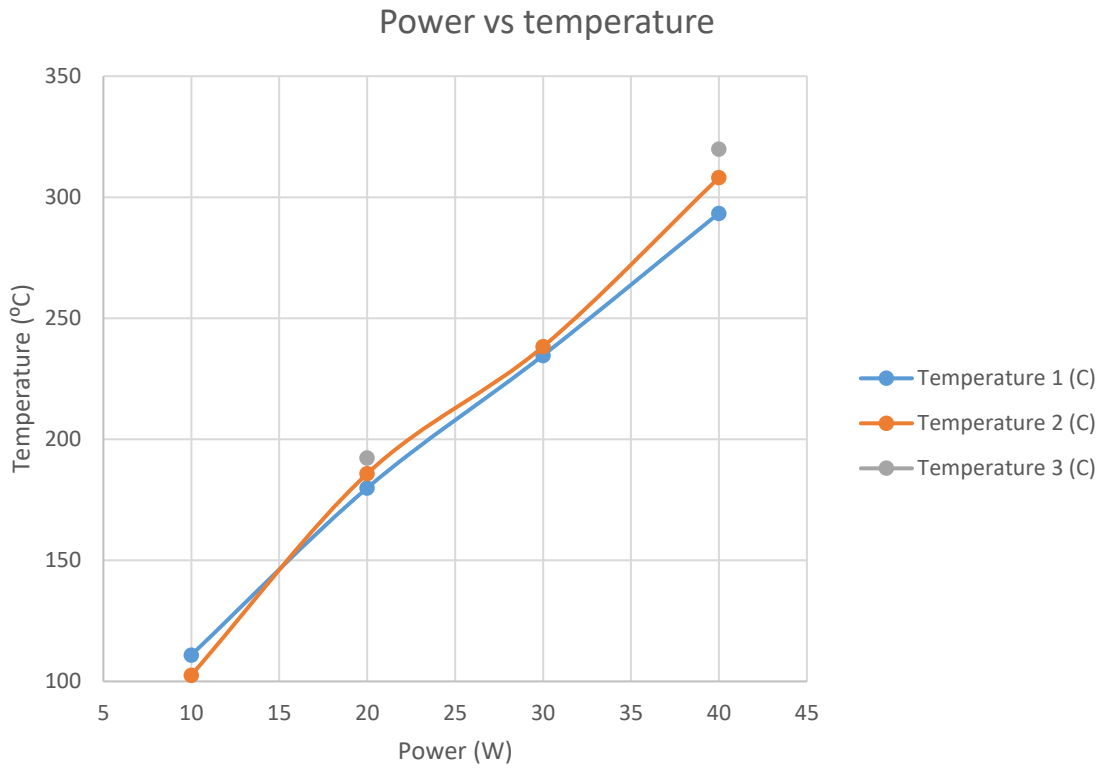


Figure 6.2 Power vs temperature graph

### 6.3 Testing completely open gap at the bottom (adding emission)

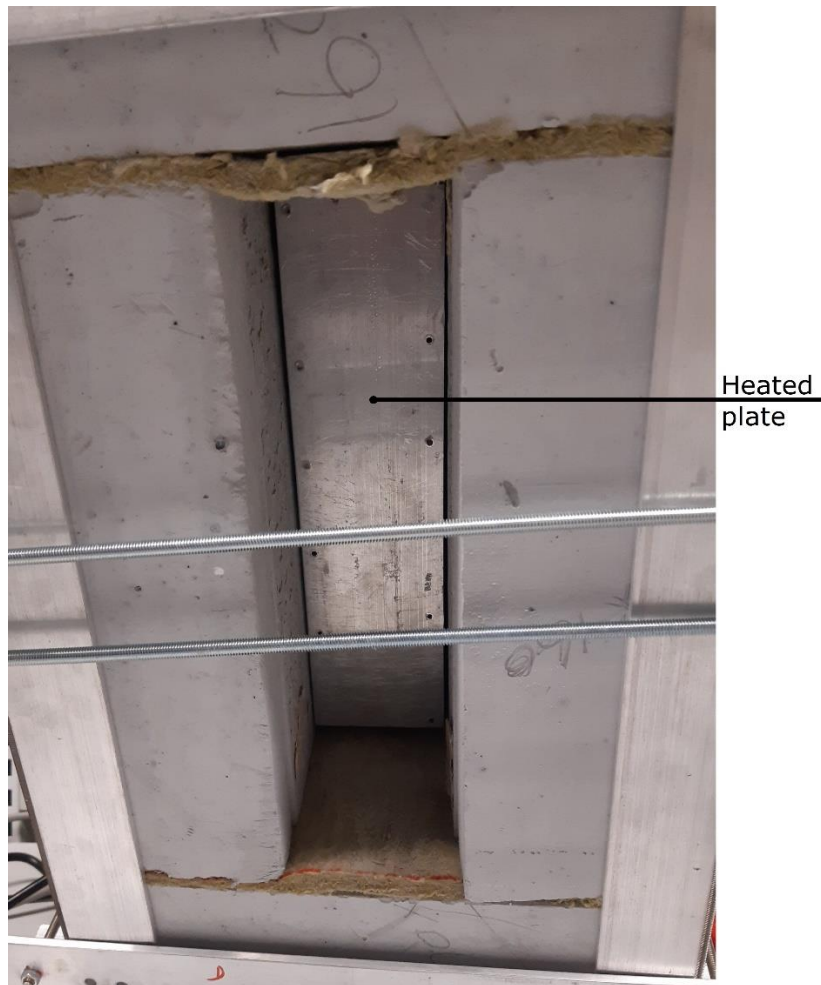


Figure 6.3 Illustration of the open gap at the bottom

In the figure above, it is illustrated that the enclosure gap at the bottom of the assembly in full width of the thermal absorber heated plate is open. The open gap at the bottom has a significant effect on the heat transfer and the power output against temperature of the heated plate.

Temperature testing of the heated plate is also obtained while keeping the heated plate open to the ambient temperature. This means that the gap of the assembly is now without any insulation material. These tests are made to compare the results with the fully closed heated plate to the heated plate which is open at the bottom. In actual TEG system, the heated plate must be at least partially open because sun rays from the parabolic dish will eventually hit the bottom of the heated plate.

In this task, the area of the opening will be decreased, and temperature tests will be obtained for the range of given inputs. The table below shows that through the open gap, a significant heat dissipates. The more input power given to the system; more heat

is dissipated into the atmosphere. Gap is in the bottom and thermal heated plate in significant depth. This means that there is be practically any convection.

Table 6.4 Fully open thermal absorber heated plate at the bottom

Fully open gap at the bottom at 90°		
S. No	Power (W)	Temperature (°C)
1.	10	104
2.	20	153
3.	30	208
4.	40	253

## **6.4 Testing completely open gap at different angles (adding convection)**

The whole assembly is tested at different angles. In order to support the assemble, a robust design should be considered. The design of extra parts should vary in height to change the angle of the assembly. Two M4 threaded studs were used with a larger base to support the assembly. Threaded studs had a possibility to support the assembly while being at different heights with the help of nuts and L-shaped part which in turn changed the angle of the assembly. In the following figure, threaded studs and L-shaped part is illustrated.

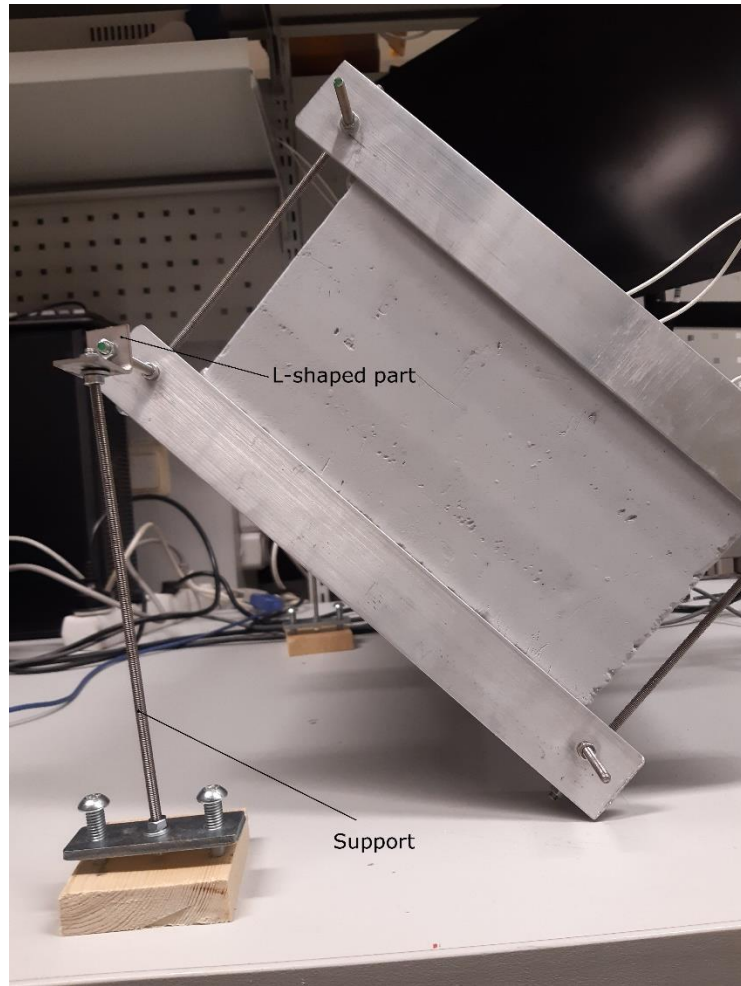


Figure 6.4 Support at different angles

Table 6.5 Fully open gap at different angles

Fully open gap at the bottom at 0°		
S. No	Power (W)	Temperature (°C)
1.	10	79
2.	20	102
3.	30	132
4.	40	160
Fully open gap at the bottom at 30°		
1.	10	94
2.	20	124

3.	30	162
4.	40	199
Fully open gap at the bottom at 45°		
1.	10	104
2.	20	144
3.	30	188
4.	40	231
Fully open gap at the bottom at 60°		
1.	10	111
2.	20	166
3.	30	211
4.	40	250

## 6.5 Partially open gap testing (emission evaluation)

Table 6.6 Partially filled gap

Partially filled gap at the bottom at 0°		
1.	10	96
2.	20	119
3.	30	157
4.	40	194



## 7 RESULTS ANALYSIS

### 7.1 Iterations to match Ansys simulations for thermal conductivity

As per the supervisor's guidelines, thermal conductivity of the insulating material has been changed in material properties in Ansys. This increase in the thermal conductivity of the material is done through an equation. Initially, the thermal conductivity  $K$  is set to the Skamotec specified value of  $0,061 \text{ W/ (m. K) }$ .

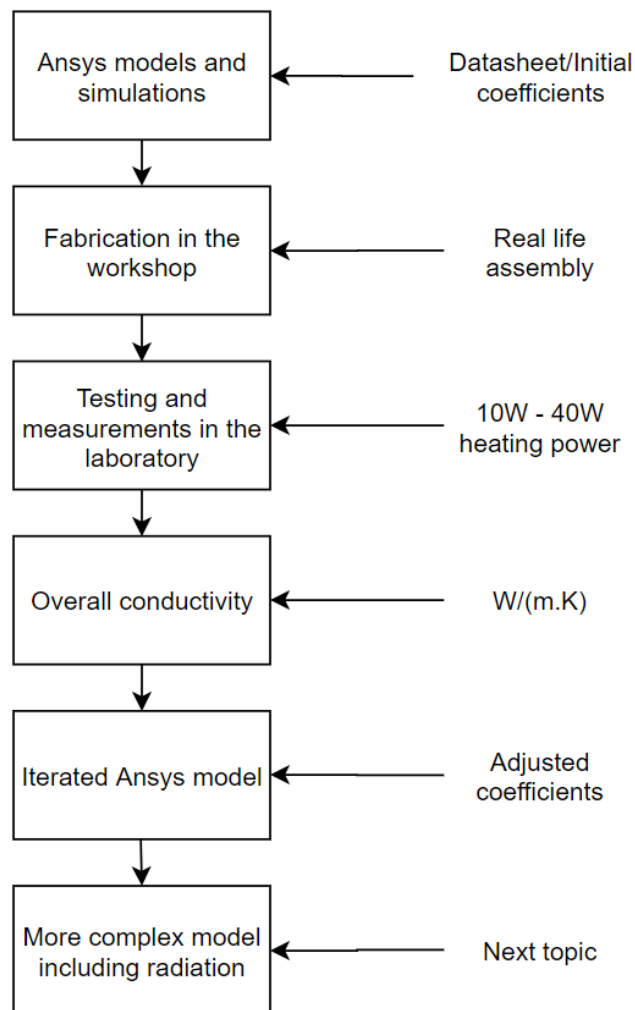


Figure 7.1 Thermal conductivity specification flow chart

The iteration is done by multiplying the ratio of power of the prototype to the power of the heated plate in Ansys for a specific temperature.

$$K = \frac{P_{Real}}{P_{Ansys}} * K_{initial} \quad (7.1)$$

where K is thermal conductivity

$P_{Real}$  is power input to the prototype in the laboratory

$P_{Ansys}$  is the power of the heated plate in Ansys

Following the equation 7.1, calculations have been done by just substituting the values in it. The table below shows power of the prototype, Ansys and changed Ansys result for two different values of temperatures.

Table 7.1 Prototype power vs Ansys power for thermal conductivity

S. nr	$P_{real}$ (W)	$K_1$ (W/(m·K))	$P_{ansys 1}$ (W)	$K_{real}$ (W/(m·K))	$P_{ansys 2}$ (W)	Temperature (°C)
1.	10	0,06	5	0,12	10	103
2.	20	0,06	11	0,12	20	186
3.	30	0,06	15	0,12	30	238
4.	40	0,06	20	0,12	40	308

From the table above, it is clearly illustrated that the Ansys power input gets approximately equal to the real power input in its first iteration.  $P_{ansys 1}$  is the Ansys power input result after simulating it on the software using the initial thermal conductivity.  $P_{ansys 2}$  is the power input after iterating the thermal conductivity of the material and changing the engineering data in Ansys. In comparison with the thermal conductivity given by the material does not correspond to the accurate input power. This means that the real thermal conductivity of the material is much higher than the given in the data sheet of the material. These results are obtained by taking the measurement of the table 6.2 into account. This proves that the material and assembly of the design in the real application has a different thermal conductivity.

## 7.2 Iterations in Ansys simulations for emissivity

As thermal conductivity of the material has been iterated, emissivity of the material is also taken into account. Radiation or thermal radiation is basically electromagnetic radiation which lies on the range of both, visible radiation (light) and infrared radiation

which human being cannot see with their eyes. It is also a mode of heat transfer which also travels in space. One of the examples of radiation is heat energy coming from sun. Emissivity is the ratio of radiation from the observed surface to the radiation from an ideal black body at the same given temperature. The value of emissivity varies from 0 to 1. It has been calculated that the thermal radiation emitting from an ideal or perfect black body (having emissivity of 1) is equal to the rate of approximately 448 watts per square metres at the room temperature. In real life, all material objects have emissivity less than 1 and emits at comparatively lower rate than ideal black body.

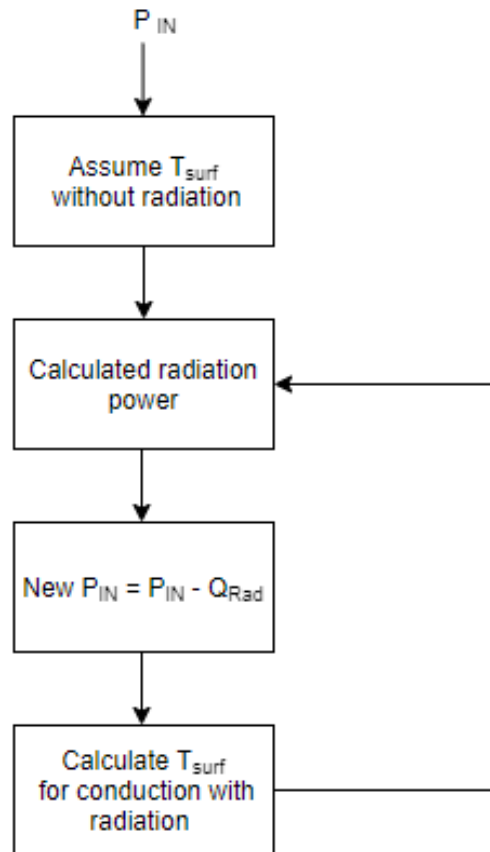


Figure 7.2 Emissivity flow chart

Comparison and actual emissivity finding is done in Excel using iterative algorithm in Excel. Emissivity true results are presented in Table 7.2.

Table 7.2 Prototype power vs Ansys power for emissivity

S. nr	$P_{real}$ (W)	Emissivity, $\epsilon$	$P_{ansys\ 1}$ (W)	Emissivity, $\epsilon$	$P_{ansys\ 2}$ (W)	Temperature ( $^{\circ}C$ )
1.	10	0,02	5	0,2	10	104
2.	20	0,02	12	0,2	20	153

3.	30	0,02	18	0,2	30	208
4.	40	0,02	26	0,2	40	253

### 7.3 Iterations for thermal convection coefficient

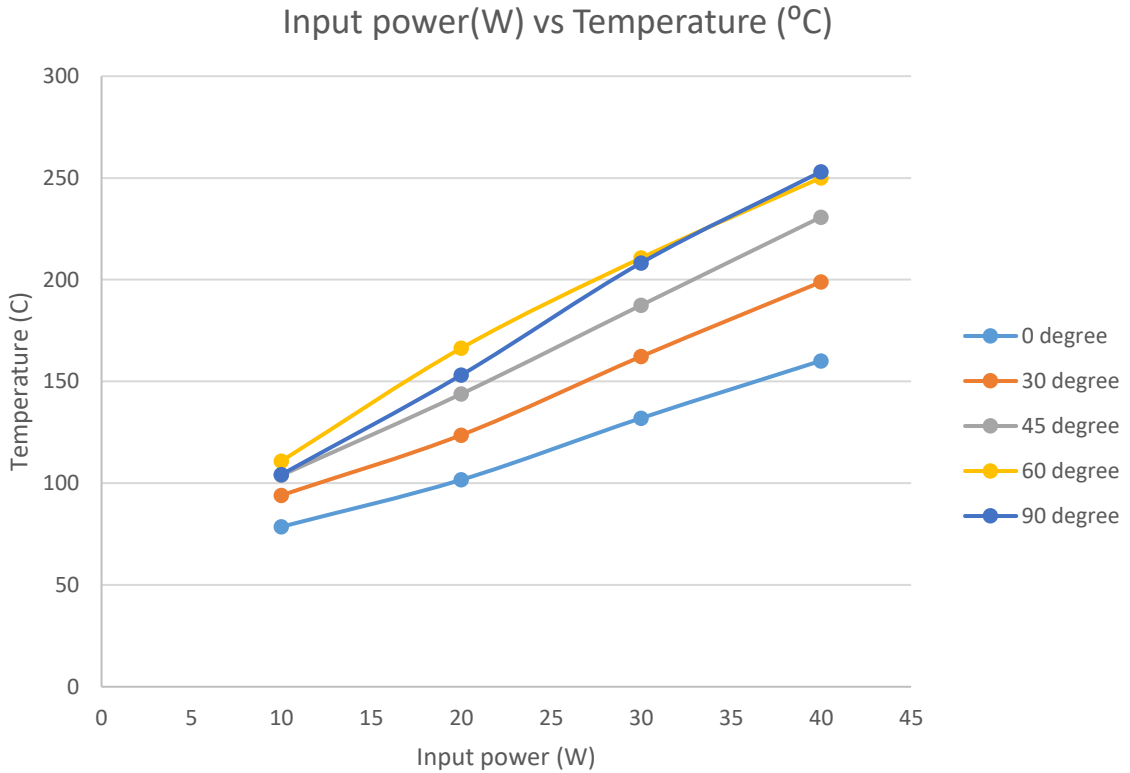


Figure 7.3 Trend x and trend constant of heat transfer at angles

W	10	20	30	40	Trend x	Trend constant
0°	79	102	132	160	2,7	49,0
30°	94	124	162	199	3,5	56,5
45°	104	144	188	231	4,0	60,4
60°	111	166	211	250	4,6	69,0
90°	104	153	208	253	5,0	54,0

Graph in the figure 7.3 clearly illustrates that the heat transfer is inversely proportional to the applied angle. This means that when the open cavity of the enclosure faces downwards, the heat transfer decreases. With the increase in the angle, the open cavity starts to move downwards, which in turns decreases the heat transfer from the heated plate and increases the temperature. The tests were performed at the angles of 0, 30, 45, 60, and 90.

## **8 TEG ADAPTER PROPOSAL**

Absorber is one of an essential part in the whole assembly. It is an essential part because this is a part which touches a TEG. The hot side of the TEG sit on the hot side of the adapter and the cold side sit on the cold side of the adapter. This part is of the whole assembly is redesigned, in a way that the hot side plate stays away from the cold side of the TEG as much as possible. To redesign the absorber, the shape like an hourglass is considered. The shape of an hourglass is like two conical shaped bodies are joined together vertically. On the empty side around the absorber is filled with the calcium silicate insulation material. This insulating material also helps to optimize the design and increase efficiency and keep the temperature of the hot side of the adapter high.

### **8.1 Previously used adapter**

Previously, the absorber was only two plates sandwiched between a TEG. Those two flat plates were also bigger in size then the size of the TEG. Through previous design, more thermal energy used to travel through the hot plate to the cold plate via convection, conduction, and radiation as well. One of the reasons for more heat travel was due to the exposed surfaces of the plates to each other. The other reason for more heat transfer is due to the fact that both these plates were parallel to each other, and it is proven through basic heat and mass transfer equations that the bodies parallel to each other transfers more thermal energy then the bodies on an angle.

### **8.2 Adapter redesigned**

The adapter is redesigned in solidworks. In solidworks, loft command is used to extrude the desired shape of an hourglass. In between two conical shaped bodies, TEG is also placed in the 3D model. The top cone is cold side, and the bottom cone is hot side of the adapter. These both cones are intact to the respective sides of the TEG. Material of the adapter is also considered to optimize. It is desired to keep a material on hot side of the absorber so that it may have less thermal conductivity while on the other side of the absorber which is a cold side, it is desired to have maximum thermal conductivity so that the temperature on the cold side remains low. For hot side of the adapter, brass is used because it has low thermal conductivity and for the other side, copper is used because of the high thermal conductivity.

The top and bottom area of the adapter is 60x60mm, which decreases to 40x40mm. The area decreases to 40x40mm because the TEG used in the laboratory is of this area. The TEG sits perfectly with the adapter's top and bottom parts. In the picture below the blue colour side is of the cold side where the surface in red colour is the hot side of the absorber.

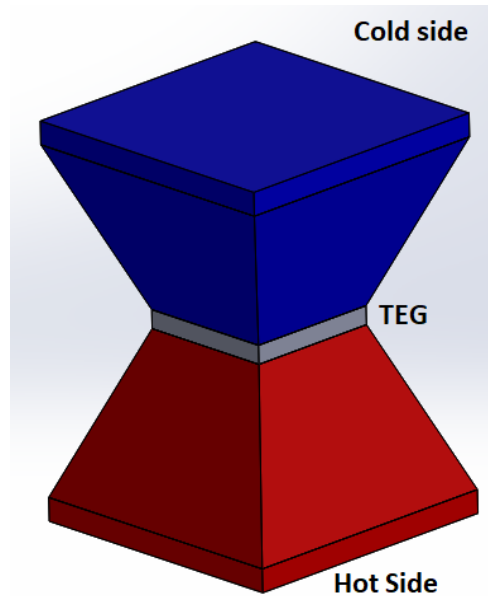


Figure 8.1 Absorber

### 8.3 Adapter simulation

Likewise absorber, TEG's adapter is also centre of consideration for the design optimization. In order to optimize the adapter's design, simulations with same boundary conditions were applied in Ansys. Initially, rectangular plates were installed around the calcium silicate insulation material and has been simulated. In between those two rectangular plates, a TEG is sandwiched in Ansys. In the picture below, the top part is a cross section of rectangular plates and a TEG wrapped around insulation material. The bottom part is the simulation of the top part of the picture. It is clear that the temperature which is applied on the bottom surface does not reaches the TEG in an optimum manner. It has also been observed that the temperature contours are of a shape of an hourglass. The rectangular shape of the top and bottom plates was changed to the cone shape and was being simulated.

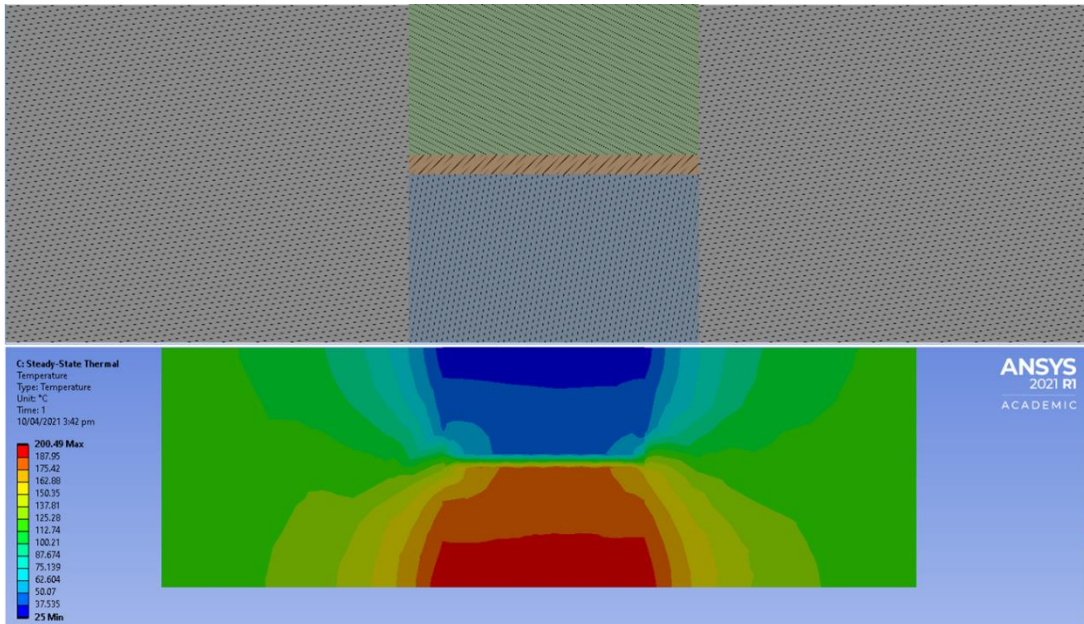


Figure 8.2 Rectangular plates

In the picture below, the cone shaped top and bottom plates were simulated. The simulation clearly shows that through the shape change, the temperature on both the side reaches the TEG in an optimum manner. The red and blue contours are almost the same on TEG surface as on the topmost and bottom surfaces.

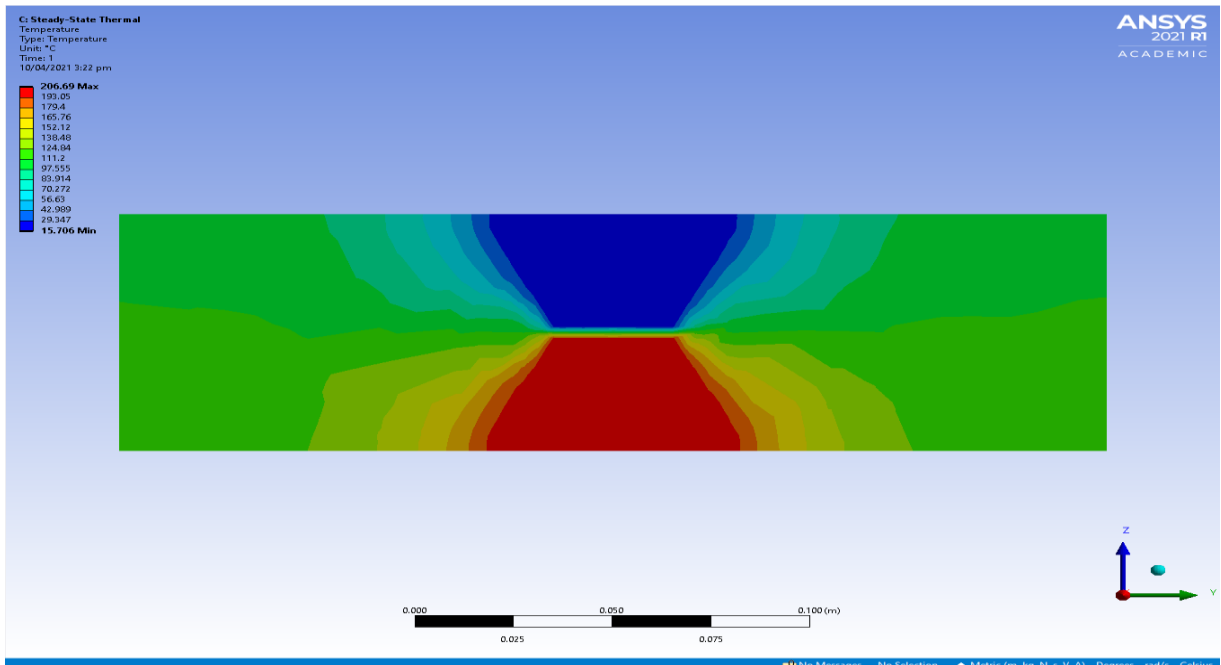


Figure 8.3 Cone shaped plates



## 9 CONCLUSION

In the current study of the thermoelectric generator thermal collector, the design of the assembly has been optimized. The main aim in this thesis was to achieve such a design that the thermal energy on the hot side sinks to the cold side as less as possible.

In order to achieve the goal, simulations were performed, initially. These simulations were done in Ansys for the thermal calculations using finite element method. Properties of the insulating material used in the fabrication was also used in the material properties of the simulation to get the accurate results. After simulating several 3D models in different orientations and configurations, a final and optimum design was proposed to fabricate.

The fabrication of the whole assembly was done in the workshop of the university. Calcium silicate material was used as an insulation of the heated part. This small and rectangular insulating material was joined together with the thermal glue. This glue can easily handle high temperature and can keep parts intact. Resistance heaters were installed on the heated plate of the assembly and temperature sensors were set on the heated plate to measure the temperature of the plate.

After the fabrication, testing of the assembly was performed by applying different input powers. While testing the model with different input powers it was observed that the results obtained from the simulations were not perfectly the. These differences in the readings were due to the heat leakages in the real model and ideal boundary conditions in the simulations. The results in the simulations had better efficiency than the results obtained through physically testing the prototype. This corresponds to the expected results of real system which is lower than the materials' ideal values-based estimations.

Future scope in this research is to install proposed TEG adapter in this assembly with a working TEG module installed on it as well. The TEG, which will be sandwiched in between the proposed adapter will be providing electrical power production output results.

## 10 JÄRELDUSED

Käesolevas termoelektrilise generaatori jaoks sobiliku soojuskollektori uuringus on kujundatud optimeeritud koost. Selle töö peamine eesmärk oli jõuda sellise kujunduseni, millisel oleks vähim soojusleke termoelektrilise generaatori kuumalt poolelt külmale.

Eesmärgi saavutamiseks alustati imitatsioonide läbiviimisega. Need soojusarvutused teostati lõplike elementide meetodil Ansysi tarkvaral. Isolatsioonimaterjali arvutustulemustel omandatud parameetreid rakendati ka simulatsioonikeskkonnas, et parandada tulemuste täpsust. Peale simulatsioone 3-mõõtmeliste mudelitega erinevates suundades ja seadistuses pakuti välja katsetusteks sobilikuim optimaalne kujundus.

Koost valmistati ülikooli töökodades. Kuumenevate osade soojusisolatsioonimaterjaliks oli kasutusel kaltsiumsilikaat. See isolatsioonimaterjal liideti kokku kuumakindla liimiga. Selline liim talub hästi kuumust ja hoiab detaile kindlalt. Takistuslikud kuumutuselemendid paigaldati kuumutatavale osale ja lisaks paigaldati temperatuuriandurid erineva kuumutatava plaadi punktidesse temperatuuri mõõtmiseks.

Koostu valmistamise järel katsetati koostu erinevate küttevõimsuste rakendamise teel. Mudeli katsetamisel erinevate sisendvõimsustega tuvastati, et simulatsioonil saadud tulemused ei olnud täielikult kokkulangevad. Tulemuste erinevused olid tingitud reaalse koostu soojusleketest ja simulatsioonikeskkonna piiritingimuste ideaalsusest. Simulatsioonidel saadud tulemused olid näitasid suuremat tõhusust kui reaalse koostu prototüübil saadud tulemused. See on reaalse süsteemi vaates ootuspärane tänu reaalse süsteemi erinevatele tunnussuurustele võrreldes materjalide ideaalsete parameetrite ja ideaalsel koostul põhinevatele hinnagutele.

Antud uuringu tulevikusuunaks on termoelektrilise elemendi liitekomponendi paigaldamine koos töötava termoelektrilise mooduliga. Termoelektriline moodul paigaldatakse käesolevas töös välja pakutud liitekomponendi poolte vahele ja võimaldab leida elektrienergia tootmisnäitajad

## LIST OF REFERENCES

- [1] E. Weston, "Apparatus for utilizing solar radiant energy". Patent 389, 124, 1888.
- [2] M. L. Severy, "Apparatus for generating electricity by solar heat". Patent 527, 379, 1894.
- [3] M. L. Severy, "Apparatus for mounting and operating thermopiles". Patent 527, 377., 1894.
- [4] W. W. Coblenz, "Thermal generator". Patent 1077, 219., 1913.
- [5] D. Ji et al., "Thermoelectric generation for waste heat recovery: Application of a system level design optimization approach via Taguchi method," *Energy Convers. Manag.*, vol. 172, no. April, pp. 507–516, 2018.
- [6] A. Subasi, B. Sahin, and I. Kaymaz, "Multi-objective optimization of a honeycomb heat sink using Response Surface Method," *Int. J. Heat Mass Transf.*, vol. 101, pp. 295–302, 2016.
- [7] D. Kraemer, "High-performance flat-panel solar thermoelectric generators with high thermal concentration," *Nat. Mater.*, pp. 10, 532–538., 2011.
- [8] G. Chen, "Theoretical efficiency of solar thermoelectric energy generators," *J. Appl. Phys.*, no. 109, 104908., 2011.
- [9] K. McEnaney, D. Kraemer, and Z. Ren, "Modeling of concentrating solar thermoelectric generators," *J. Appl. Phys.*, no. p110, 2011.
- [10] J. Yu, Q. Zhu, L. Kong, H. Wang, and H. Zhu, "Modeling of an integrated thermoelectric generation–Cooling system for thermoelectric cooler waste heat recovery," *Energies*, vol. 13, no. 18, 2020.
- [11] M. Sajid and I. Hassan, "An overview of cooling of thermoelectric devices," *Elsevier*, pp. 15-22, 2017.
- [12] M. L. Olsen et al., "A high-temperature, high-efficiency solar thermoelectric generator prototype," *Energy Procedia*, vol. 49, pp. 1460–1469, 2014.
- [13] G. Muthu, S. Shanmugam, and A. R. Veerappan, "Solar parabolic dish thermoelectric generator with acrylic cover," *Energy Procedia*, vol. 54, pp. 2–10, 2014.
- [14] P. Li, L. Cai, P. Zhai, X. Tang, Q. Zhang, and M. Niino, "Design of a concentration solar thermoelectric generator," *J. Electron. Mater.*, vol. 39, no. 9, pp. 1522–1530, 2010.

- [15] R. K. Nayak, "Effect of angle of attack and wind direction on limiting input heat flux for solar assisted thermoelectric power generator with plate fin heat sink," in *Solar Energy* 186, 2019.
- [16] A. Date, C. Dixon, R. Singh, and A. Akbarzadeh, "Theoretical and experimental estimation of limiting input heat flux for thermoelectric power generators with passive cooling," *Sol. Energy*, vol. 111, pp. 201–217, 2015.
- [17] B. Sinha, *Study of Solar Thermoelectric Generators Coupled with Concentrated Solar Power Systems*, San Francisco, California, January 2017.
- [18] L. Lin, Y. F. Zhang, H. B. Liu, J. H. Meng, W. H. Chen, and X. D. Wang, "A new configuration design of thermoelectric cooler driven by thermoelectric generator," *Appl. Therm. Eng.*, vol. 160, no. July, p. 114087, 2019.
- [19] N. Sendhil Kumar and K. S. Reddy, "Numerical investigation of natural convection heat loss in modified cavity receiver for fuzzy focal solar dish concentrator," *Sol. Energy*, vol. 81, no. 7, pp. 846–855, 2007, doi: 10.1016/j.solener.2006.11.008
- [20] A. J. G. Yunus A. Cengel, *Heat and mass transfer fundamentals and applications*.